Gene expression profile underlying neuronal survival and functional recovery by very early exposure to an enriched environment after hypoxic-ischemic brain injury

Hoo Young Lee

Department of Medicine

The Graduate School, Yonsei University

Gene expression profile underlying neuronal survival and functional recovery by very early exposure to an enriched environment after hypoxic-ischemic brain injury

Hoo Young Lee

Department of Medicine

The Graduate School, Yonsei University

Gene expression profile underlying neuronal survival and functional recovery by very early exposure to an enriched environment after hypoxic-ischemic brain injury

Directed by Professor Jung Hyun Park

The Doctoral Dissertation
submitted to the Department of Medicine,
the Graduate School of Yonsei University
in partial fulfillment of the requirements for the degree of
Doctor of Philosophy in Medical Science

Hoo Young Lee

December 2021

This certifies that Doctoral Dissertaion of
Hoo Young Lee is approved

Theses Supervisor: Jung Hyun Park

Thesis Committee Member #1: Sung-Rae Cho

Thesis Committee Member #2: Lark Kyun Kim

Thesis Committee Member #3: Se Hoon Kim

Thesis Committee Member #4: Sung Hoon Kim

The Graduate School
Yonsei University

December 2021

Acknowledgements

There was a lot of help of many people until this doctoral dissertation was completed. I would like to express my gratitude to them through this page.

First of all, I would like to express my sincerest appreciation to Professor Jung Hyun Park, thesis supervisor. He has always given warm and thoughtful advices on the life as a rehabilitation doctor as well as suggestion and encouragement of this thesis.

I would like to take this opportunity to extend my profound gratitude to Professor Sung-Rae Cho and his colleagues who fulfilled the experiments. Without their dedication, this paper could not have been completed.

I truly appreciate thesis committee members, Professor Lark Kyun Kim, Professor Se Hoon Kim and Professor Sung Hoon Kim. Their thoughtful suggestions and insights have made this project more valuable and enriched.

I also appreciate unsparing advices of Professor Byung-Mo Oh, Professor Won Seok Kim, Professor Tae-Woo Kim, Professor Seung Don Yoo, Professor Jang Woo Lee and Professor Ja Young Choi.

Lastly, I can't thank enough to my family, especially my mother, Jung Hee Kim, who has been heartily devotional, my husband Jeongwan Kang, who has always been by my side and a delightful lovely son, Dong Hoon, who is always invigorating.

Table of Contents

LIST OF FIGURES

LIST OF TABLES

Abstract

Gene expression profile underlying neuronal survival and functional recovery by very early exposure to an enriched environment after hypoxic-ischemic brain injury

Hoo Young Lee

Department of Medicine
The Graduate School, Yonsei University

(Directed by Professor Jung Hyun Park)

Stroke is a leading cause of mortality and serious long-term disability. Early rehabilitation is an effective strategy for stroke treatment; however, studies demonstrated that very early forced mobilization was associated with poorer outcomes. Apoptosis plays a critical role after stroke. Recent studies have shown an increase in the levels of Fas and FasL expression in the brains of animal models of stroke and in patients with ischemic stroke in hyperacute phase. Exposure to enriched environment (EE) including complex combinations of a running wheel for voluntary exercise, cognitive, and social stimuli, has been shown to improve therapeutic outcomes in rodents. However, the functional recovery via regulation of Fas/FasL-mediated apoptosis of genes in hyperacute phase of ischemic stroke has yet to be reported. The aim of the study is therefore to determine whether hyperacute exposure to EE can regulate Fas/FasL-mediated apoptosis in cerebral cortex and hippocampus following hypoxic-ischemic brain injury and improve neuronal survival and neurobehavioral function.

Adult C57Bl/6 mice were subjected to permanent hypoxic-ischemic brain

injury by unilateral ligation of right carotid artery under hypoxia (8% oxygen). A total of 70 C57Bl/6 mice aged 6 weeks were randomly assigned to either hyperacute EE or standard cage (SC) (n = 35 per group) within 3 hours after exposure to hypoxic-ischemic brain injury for 2 weeks. A total of 40 six-week-old C57Bl/6 mice were randomly assigned to either delayed EE or SC (n = 20 per group), 3 days after exposure to hypoxic-ischemic brain injury for 2 weeks.

In both models, open field test was performed to evaluate anxiety and locomotion. A cylinder test was performed to evaluate anxiety and hyperactivity, followed by Y-maze test to evaluate short-term spatial memory and a ladder rung walking task to evaluate locomotor function. The underlying molecular mechanisms were investigated via transcriptome analysis of differentially expressed genes in cerebral cortex and hippocampus. The effects of exposure to EE on the levels of apoptosis-associated proteins such as FAS, FADD, Bax, Bcl-2, cleaved caspase-8, caspase-8, cleaved caspase-3, and caspase-3 were analyzed via western blot. The neuroprotective mechanisms were further analyzed by measuring the infarct volume and assessing the level of terminal deoxynucleotidyl transferase dUTP nick-end labeling (TUNEL) and fas-associated death domain (FADD) staining via immunohistochemistry.

Hyperacute exposure to EE significantly improved anxiety, motor function, and cognition following hypoxic-ischemic brain damage compared with exposure to the SC. Transcriptome analysis revealed that the levels of *FADD*, *FAS*, and *CASP8* in the extrinsic pathway of apoptosis were significantly downregulated by the EE compared with the SC conditions. Western blotting analysis revealed that hyperacute exposure to EE significantly suppressed the expression of FAS, FADD, and Bax, and the ratios of Bax/Bcl-2, cleaved caspase-8/caspase-8, and cleaved caspase-3/caspase-3, and in addition to increasing the expression of Bcl-2 in the cerebral cortex and the hippocampus compared with the control group. Hyperacute exposure significantly decreased the total infarct volume relative to the control group. Immunohistochemistry showed that the

number of TUNEL-positive cells and FADD-positive neurons in the cerebral cortex and hippocampus were significantly decreased in mice exposed to EE compared with mice in SC.

Compared with SC conditions, delayed exposure to EE after hypoxic-ischemic brain damage significantly improved the levels of anxiety, motor function, and cognition. Western blot analysis showed that apoptosis was not significantly suppressed by delayed exposure to EE. Total infarct volume was significantly decreased by EE relative to the SCs. Compared with SC conditions, delayed exposure to EE significantly decreased TUNEL staining but not FADD staining in cerebral cortex and hippocampus.

Taken together, these results demonstrate the therapeutic potential of EE initiated in the hyperacute phase of stroke resulting in improved functional recovery and neuronal survival by inhibiting both extrinsic and intrinsic apoptosis. A significant downregulation of Fas/FasL-mediated apoptosis was detected in cerebral cortex and hippocampus. Therefore, hyperacute exposure to EE may enhance neuroprotection and functional recovery after ischemic stroke.

Key words: environmental environment, hypoxic-ischemic brain injury, stroke, apoptosis, FAS, death receptor, extrinsic pathway, functional recovery, hyperacute

Gene expression profile underlying neuronal survival and functional recovery by very early exposure to an enriched environment after hypoxic-ischemic brain injury

Hoo Young Lee

Department of Medicine
The Graduate School, Yonsei University

(Directed by Professor Jung Hyun Park)

I. INTRODUCTION

1. Overview of stroke

Stroke is a major cause of serious long-term disability, especially in more than 80% of all cases of ischemic attacks.[1-3] Ischemic stroke results in sudden neurologic deficit, including impaired motor response, cognition, communication, and mood, and directly reduces patients' quality of life, with a heavy burden on family and community.[4-5] Therefore, effective strategies for functional recovery of patients with stroke are imperative.

2. Inhibition of apoptosis, a promising neuroprotective rehabilitation strategy

Acute brain ischemia triggers an "ischemic cascade" of pathophysiological events such as energy failure, excitotoxicity, oxidative stress, inflammation and apoptosis, resulting in neuronal cell death. Ample evidence suggests the critical role of apoptosis in the pathophysiology of acute brain ischemia, resulting in significant loss of brain cells.[4, 6] The ischemic core of the brain experiences a

sudden reduction of blood flow, just minutes after ischemic attack with irreversible injury and subsequent cell death. However, apoptosis within the ischemic penumbra may occur after several hours or days, and may be reversible.[6, 7] Early animal and human studies revealed different apoptotic mechanisms during acute brain ischemia, as well as the efficacy of anti-apoptotic agents and inhibitors of apoptosis ameliorating brain tissue injury and reducing morbidity.[8-13] Therefore, the inhibition of apoptosis may be a promising neuroprotective rehabilitation strategy, suggesting the need to elucidate the anti-apoptotic mechanisms involved.

Ischemic stroke triggers two main pathways of apoptosis. The intrinsic pathway is initiated by the disruption of mitochondria and the release of cytochrome C, which is mediated by members of the Bcl-2 family such as antiapoptotic protein B cell lymphoma/leukemia-2 (Bcl-2) and proapoptotic protein Bcl-2-associated X protein (Bax)[7]. The extrinsic pathway is triggered by signaling cell death receptors in the plasma membrane including tumor necrosis factor (TNF)-receptor 1, apoptosis antigen-1 (APO1/Fas/CD95), and TNF-related apoptosis-inducing ligand receptor (TRAIL-R).[7, 14]

3. Significance of stroke rehabilitation targeting extrinsic apoptosis

Fas is one of the cell surface death receptors belonging to the TNF receptor superfamily. Fas ligand (FasL) binds to the Fas receptor, which triggers recruitment of the cytoplasmic adaptor protein Fas-associated death domain protein (FADD), and initiates apoptosis.[15] The “death effector domain” at the N terminus of FADD binds to procaspase-8.[16] This complex (FasL–Fas–FADD–procaspase-8), referred to as death-inducing signaling complex (DISC), is assembled within seconds of Fas receptor engagement. The DISC catalyzes the proteolytic cleavage and transactivation of procaspase-8 to generate caspase-8.[16] The activated caspase-8 is released from the DISC complex into the cytoplasm to initiate the downstream cleavage of caspase-3, which leads to the execution phase of apoptosis, resulting in nDNA damage and apoptosis.[17]

Fas, FADD and caspase-8 are strongly associated with the incidence of ischemic stroke, independent of several potential confounding factors.[18] Further, the Fas ligand/receptor signaling pathway has been suggested as a critical inducer of apoptotic signals in acute ischemia.[19-21] The first day of ischemic stroke onset is marked by significantly higher levels of serum and cerebrospinal fluid sFas/APO1 in patients with stroke than in control subjects, followed by a gradual decline.[21] Analysis of post-mortem tissues derived from ischemic stroke victims revealed the highest levels of active caspase-8 on day 1 of onset, followed by a slow decrease with time.[22] Some early studies showed that therapeutic neutralization of FasL or Fas or under-expression of FADD or caspase-8 reduced the levels of stroke-related damage and neurologic deficit in rodent models of focal cerebral ischemia.[23-25] The extrinsic pathway of apoptosis also represents a potent therapeutic target in acute traumatic brain injury, acute spinal cord injury (SCI), seizure, acute organ injury or parasite infection.[26-34] Thus, it is reasonable to hypothesize that rehabilitation targeting downregulation of Fas/FasL-mediated apoptosis in early phases of ischemic stroke leads to neuroprotection and functional recovery.

4. Optimal time of initiation and intensity of exercise required for functional recovery after stroke

The optimal time to initiate rehabilitation after stroke has yet to be established, although evidence increasingly suggests the benefit of early, organized, and interprofessional stroke rehabilitation within the first 2 weeks of stroke.[35, 36] However, increasing evidence suggests that commencing high-dose, very early mobilization within 24 hours of stroke onset may adversely affect patient outcomes.[37-42] Most clinical and preclinical studies investigating exercise-induced effects after stroke utilized the forced exercise (FE) paradigm. The results of A Very Early Rehabilitation Trial after stroke (AVERT) trial demonstrated that high-dose and forced mobilization protocol within 24 hours of stroke onset was less

favorable than the usual care.[39] In experimental models of animal stroke, FE in hyperacute phase exacerbated brain damage, increased apoptotic cell death, and delayed functional recovery.[43-47] However, the effects of hyperacute exposure to environmental enrichment (EE), including voluntary exercise (VE), on neuroprotection and functional recovery have yet to be fully investigated. In contrast to previous studies, the current study focuses on the effects of exposure to EE on the inhibition of apoptosis during hyperacute phase of ischemic stroke.[48]

5. EE as a model of rehabilitation in animal study

The experimental animal model of EE evaluates social interaction, stimulation of exploratory behavior with objects such as toys and a set of tunnels, and a running wheel for voluntary exercise.[49,50] Furthermore, EE is a non-invasive approach based on voluntary physical activity and non-stressful conditioning.[51] While most of the studies investigating the potential mechanisms underlying the neuroprotective effect of EE focused on neurogenesis, synaptogenesis or angiogenesis, the importance of neuronal survival has yet to be fully elucidated.[52-55] Few studies delineated the mediating effect of EE on extrinsic apoptosis in an experimental stroke model.

6. Aims of this study

The study sought to determine the neuroprotective effects of hyperacute exposure to EE following hypoxic-ischemic brain injury and compare the mechanisms associated with delayed exposure to EE in adult mice. We focused on the effects of altered expression of apoptosis-related genes on neuronal survival and functional recovery and explored novel neuroprotective rehabilitation strategies after stroke.

Ⅱ. MATERIALS AND METHODS

1. Construction of an adult hypoxic–ischemic (HI) brain injury model

Ischemic brain damage was induced in 6-week-old C57BL/6 mice via unilateral right carotid artery ligation under anesthesia with a mixture of ketamine and xylazine (Rompun). Hypoxic brain injury (8% O_2 for 30 minutes) was also generated as previously described.[56] Visual inspection of the wide-field microscopic images was used to assess the severity of brain injury.

2. Experimental procedures and cage condition

To establish a hyperacute EE model, a total of 70 C57BL/6 mice were randomly housed in standard cages (SC) or very early EE (n = 35 per group) within 3 hours of exposure to hypoxic-ischemic brain injury for 2 weeks. In order to develop a delayed EE model, a total of 40 C57Bl/6 mice were randomly assigned to either delayed EE or SC (n = 20 per group), 3 days after exposure to HI brain injury for 2 weeks.

The EE mice were housed in a large cage (86 × 76 × 31 cm^3) containing novel objects, such as tunnels, shelters, toys, and running wheels for VE and social interaction (12-15 mice/cage) (Figure 1A), whereas the control mice were housed in SCs (27 × 22.5 × 14 cm^3) without social interaction (3-4 mice/cage) (Figure 1B). The brain regions were dissected based on the gross anatomy of the mouse brain atlas, and the stereotaxic coordinates of the cerebral cortex and hippocampus were (ML = −1.0, AP = 0.1, DV = 1.0) and (ML = −1.0, AP = −2.0, DV = 2.0), respectively. All experiments were performed with C57BL/6 mice housed in a facility accredited by the Association for Assessment and Accreditation of Laboratory Animal Care (AAALAC) and provided with food and water ad libitum under alternating 12-h light/dark cycles, according to animal protection regulations. The experimental procedure was approved by the Institutional Animal Care and Use Committee (IACUC) of Yonsei University Health System (permit number:2021-0182).

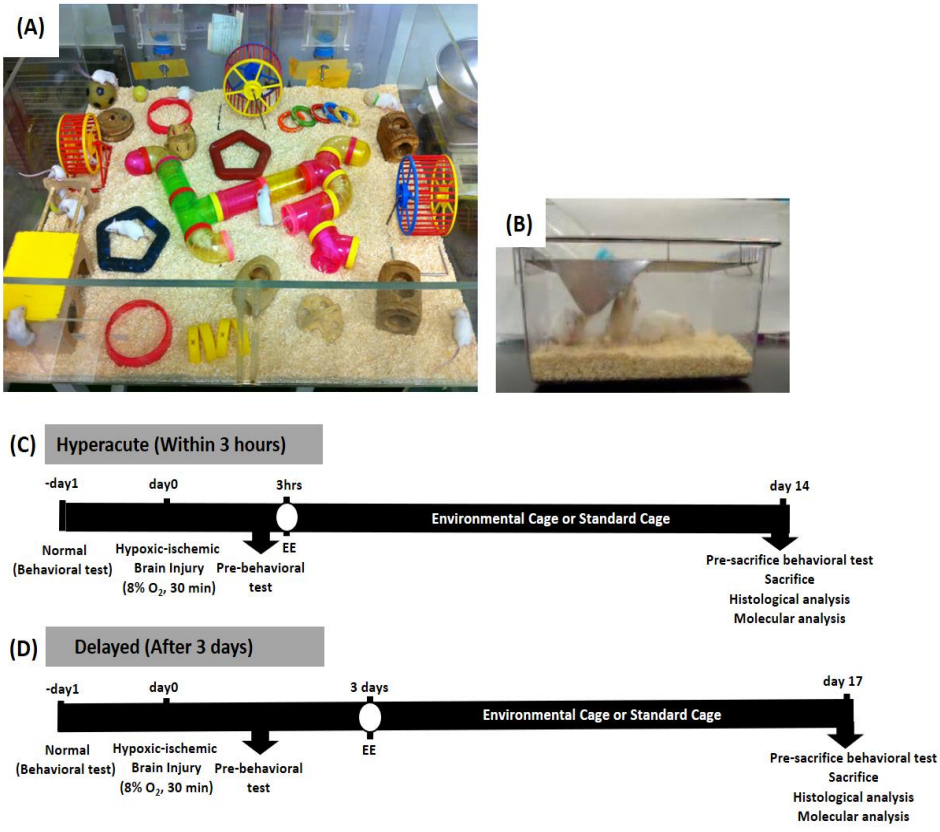

Figure 1. Experimental design. (A) Enriched environment in cages measuring 86 × 76 × 31 cm^3 including tunnels, shelters, toys, running wheels for VE, and social interaction. (B) Standard cage (27 × 22.5 × 14 cm^3) without any novel objects. (C) A schematic representation of the experimental schedule for the hyperacute EE model. A total of 70 mice with HI brain injury were randomized into 2 groups (hyperacute EE, N = 35; hyperacute control, N = 35) (D) A schematic experimental schedule involving delayed EE model. A total of 40 mice with HI brain injury were randomly divided into 2 groups (delayed EE, N = 20; delayed control, N = 20). Brain tissues were harvested for transcriptome analysis to visualize the differential gene expression.

3. Behavioral assessments

The neurobehavioral function of all mice was tested. The cylinder test, open field test, ladder walking, and Y-maze tests were performed before surgery and 14 days after exposure to EE or SC conditions (Figure 2).

A. Cylinder test

The cylinder test is designed to assess anxiety in the rodent stroke model.[57] Mice placed in a transplant plexiglass cylinder measuring 8 cm in diameter and 18 cm in height stood spontaneously and used their forepaws for support. In this test, the number of mouse forelimbs touching the wall of the cylinder (Jeung Do B&P, Seoul, Korea) was counted in the standing position over a period of 5 min.[58]

B. Open field test

Open field test is generally used to evaluate locomotor activity and anxiety in a novel environment.[58,59] Activity was monitored in an area measuring 30×30.5×31 cm^3. The floor was divided into 16 sectors. The 4 inner sectors were marked as the center, while the 12 outer sectors were defined as the periphery. Mice were placed individually in the periphery of the area and explored freely for 25 minutes, while being monitored with a video camera. The total distance traveled by each mouse was recorded for 25 min as an index of hyperactivity.[60] The resulting data were analyzed using the Smart Vision 2.5.21 (Panlab, Barcelona, Spain) video tracking system.

C. Ladder rung walking test

The ladder rung walking task can be used to distinguish subtle disturbances in motor function based on qualitative and quantitative analyses of skilled walking.[61] The ladder rung walking test was performed before and 2 months after the condition. During the test, the mice were required to walk three times for one meter on a horizontal ladder equipped with metal rungs (Jeung Do B&P) located at various distances. The number of slips from the transverse rungs with each

forelimb were measured with a videotape.[61,62]The control and EE groups among normal and HI mice were compared by measuring the difference in the percentage of slips on the transverse rungs of the ladder relative to the total number of steps taken by each forelimb, compared with the control groups.

D. Y-maze test

Y-maze test is used to evaluate cognition and short-term spatial memory.[63] This test was carried out in an enclosed Y-shaped maze (Jeung Do B&P). Normal mice tend to visit the arms of the maze one after the other. This behavior is called spontaneous alteration and used to assess short-term spatial memory in a new environment.[63] The number of each arm entries, spontaneous alterations, and percent alterations were recorded for 8 min. The percent alteration was calculated as follows: [Number of spontaneous alterations/(Number of total arm entries − 2)] × 100. At the end of each trial, the urine and feces on the maze were cleaned with 70% ethanol.

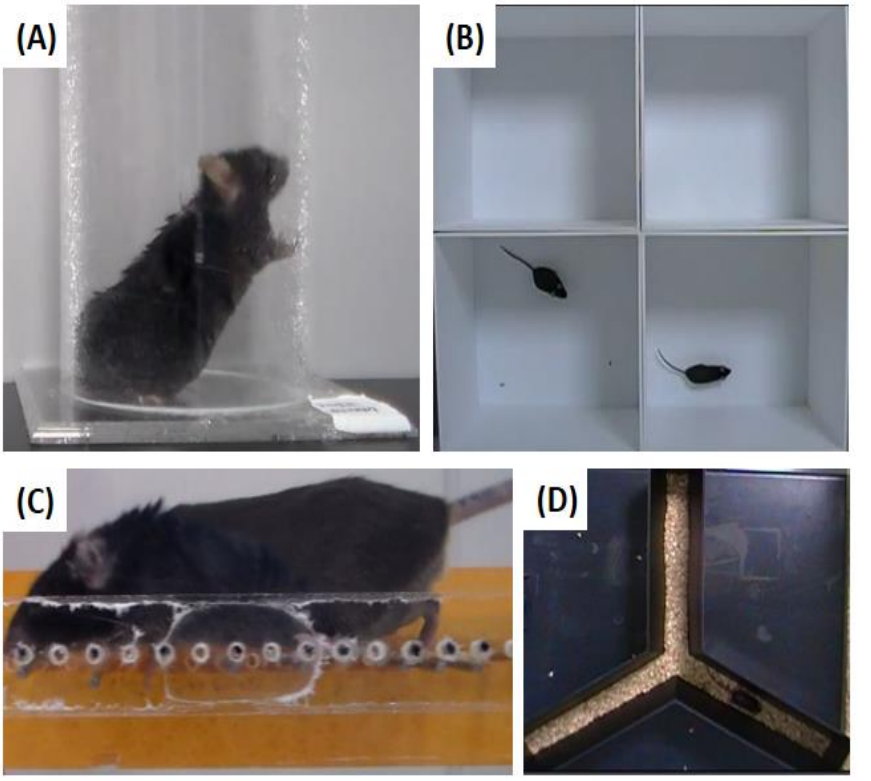

Figure 2. Neurobehavioral evaluation of HI mouse model. (A-D) Schematic representation of the cylinder test, open field test, ladder rung walking test, and Y-maze test. Anxiety and hyperactivity of the mice were assessed via cylinder (A) and open field (B) tests. The motor function was evaluated using ladder walking test (C). The Y-maze test was used to assess cognition and short-term spatial memory (D).

4. Transcriptome analysis

A. RNA preparation

Total RNA was prepared from cerebral cortex and hippocampus using the TRIzol reagent (Invitrogen Life Technologies, Carlsbad, CA, USA) according to the manufacturers' protocols. For quality control, RNA quality and quantity were evaluated via 1% agarose gel electrophoresis and the ratio of absorbance at 260

and 280 nm was determined with a Nanodrop spectrophotometer (Thermo Fisher Scientific, Waltham, MA, USA).

B. RNA sequencing and transcriptome data analysis

RNA sequencing was performed by Macrogen Inc (Seoul, Korea). The mRNA was transcribed into a library of templates. The successive cluster generation using the reagents was achieved using the Illumina® TruSeq™ RNA Sample Preparation Kit.[64-66] We performed the transcriptome analysis via RNA-seq and data handling procedures. The detailed RNA-seq protocol was performed according to the manufacturer's instructions. First, the TruSeq mRNA library construction was accomplished in 8 steps: mRNA purification and fragmentation, synthesis of first-strand cDNA, synthesis of second-strand cDNA, end repair, single 3' adenylation, ligation of adapters, enrichment of DNA fragments, followed by validation of enriched library.

C. Gene ontology and pathway analyses

Gene ontology (GO) is widely used to describe protein function in a standardized format. GO analysis of the identified proteins was performed using the Database for Annotation, Visualization and Integrated Discovery (DAVID) software (http://david.abcc.ncifcrf.gov/).[66-68] Functional annotation clustering was used to identify enriched GO terms for biological process, molecular function and cellular components to obtain an overview of the main biological processes involving these proteins. In addition, we also performed pathway enrichment analysis using the Kyoto Encyclopedia of Genes and Genomes (KEGG) pathway.

5. Molecular analysis

A. Western blot

For each sample, 50 μg of total protein and a pre-stained protein-weight marker (Bio-Rad) were separated on a 10% SDS-PAGE gel and transferred onto a PVDF

membrane (0.45 μm, Millipore) in Tris-glycine buffer with 20% (vol/vol) methanol. The membrane was blocked in 5% nonfat milk powder prepared in Tris-buffered saline containing 0.1% Tween 20 for 2 hours at room temperature, followed by incubation with primary antibodies overnight at 4°C. Anti-FAS (Abcam, Cambridge, UK), anti-FADD (Santa Cruz, Dallas, TX, USA), anti-caspase-8 (Cell Signaling Technology (CST), Danvers, MA, USA), anti-cleaved caspase-8 (CST, Danvers, MA, USA), anti-caspase-3 (CST, Danvers, MA, USA), and anti-cleaved caspase-3 (CST, Danvers, MA, USA) were the primary antibodies used at a 1:1,000 dilution. After several washes with Tris-buffered saline containing 0.1% Tween 20, the membranes were incubated with an anti-rabbit horseradish peroxidase-conjugated secondary antibody (Abcam, Cambridge, UK) diluted 1:3,000 for 2 hours. The signals were detected by chemiluminescence with Clarity Western ECL Substrate (Bio-Rad, Hercules, CA, USA). The same membrane was incubated with the β-actin antibody as an internal control.

6. Histological analysis

A. Tissue preparations

The animals were sacrificed and perfused with 4% paraformaldehyde. The harvested brain tissues were cryo-sectioned at 16-μm thickness along the coronal plane and stained with hematoxylin-eosin (H&E). H&E staining was performed with four sections from the frontal pole to the midbrain. Additionally, the 16-μm sections were cut along the coronal and sagittal plane, and immunohistochemical staining of four sections was performed over a range of >128 μm.

B. Determination of infarct volume

A section from each of the segments above was stained with H&E to measure the infarct volume. The sections were photographed using a digital camera and analyzed using ImageJ program. The infarct volumes of the lesion were expressed

as a percentage of the volume of the control hemisphere structures using the formula [(VC-VL)/VC] ×100%, where VC is the volume of control hemisphere and VL denotes the volume of non-infarcted tissue in the lesion hemisphere. The total infarct volume of each brain was calculated as the sum of the infarct volumes of the four brain slides.

C. Immunohistochemistry

The neuroprotective effects were determined by analyzing the cerebral cortex and hippocampus in each group. Fluorometric terminal deoxynucleotidyl transferase dUTP nick-end labeling (TUNEL) assay (Promega, Madison, WI, USA) was conducted to analyze the DNA fragmentation of brain cells according to the manufacturer's protocol.[69] Images of cell death were acquired via fluorescent microscopy (LSM700) and positive cell death (μm^2) with respect to DAPI area ($/\mu m^2$) was measured using ZEN Imaging Software version 2.1 (Blue edition; Zeiss).[70] The sections of the cerebral cortex and hippocampus were stained to validate Fas/FasL pathway-related neuronal apoptosis, endogenous expression of MAP-2 (1:400, Abcam) and FADD (1:400, Santa Cruz). The sections were incubated with Alexa Fluor® 488 goat anti-rabbit (1:400, Invitrogen) and Alexa Fluor® 594 goat anti-mouse (1:400, Invitrogen) secondary antibodies, and covered with Vectashield® mounting medium with 4C, 6-diamidino-2-phenylindole (DAPI; Vector, Burlingame, CA, U.S.A.). Images of apoptotic and FADD+ cells were taken using a fluorescent microscopy (LSM700), and positive apoptotic cells (μm^2) with respect to DAPI area ($/\mu m^2$), and FADD+ cells (μm^2) with respect to MAP2+ area ($/\mu m^2$) were quantified using ZEN Imaging Software (Blue edition; Zeiss). Furthermore, the three-dimensional images of the apoptotic cells were acquired with ZEN Imaging Software version 2.1 (Blue edition; Zeiss).

7. Statistical Analysis

All data were expressed as means ± SEM. The variables among groups were analyzed using one-way analysis of variance (ANOVA) followed by post-hoc Bonferroni comparison using the SPSS statistical software program (IBM, Armonk, NY; version 25.0). The variables between the two groups were compared using Student's t-test. A p value < 0.05 was considered statistically significant.

III. RESULTS

1. Hyperacute EE model

This study investigated behavioral, histological, and molecular changes induced by hyperacute exposure to EE in adult mice subjected to HI brain injury in order to elucidate the potential therapeutic mechanisms underlying the regulation of Fas/FasL-mediated apoptosis, neuronal survival, and neurobehavioral outcomes. The experimental design of the hyperacute EE mouse model is described in Figure 1(C).

A. Hyperacute exposure to EE decreases anxiety and hyperactivity in cylinder and open field tests

Cylinder and open field tests were performed after two weeks of exposure to either an EE or SC in order to determine the effects on anxiety and hyperactivity of mice sustaining HI brain injury. In the cylinder test, the rearing count in the hyperacute EE group was significantly reduced compared with the SC controls (Figure 3A). During the 25 min of open field test, the total travel distance decreased significantly in the hyperacute EE group compared with the SC controls (Figure 3B). This indicates that EE exposure alleviates anxiety and hyperactivity in the hyperacute phase of HI brain injury.

B. Hyperacute exposure to EE improves fine motor function in ladder walking test

The ladder rung walking tests were carried out to evaluate the effects of hyperacute exposure to EE on asymmetry or fine motor function following unilateral brain damage. Hyperacute exposure to EE significantly reduced the percentage of total slips when both forelimbs were used (Figure 3C). It suggests that hyperacute exposure to EE improves asymmetrical use of forelimbs and fine motor function.

C. Hyperacute exposure to EE improves cognitive function in Y-maze test

The Y-maze test was performed to determine the role of hyperacute exposure to EE in improving cognitive function. The cognitive performance was significantly enhanced in EE mice, which was indicated by the increase in the percentage of alterations in the Y-maze test (Figure 3D).

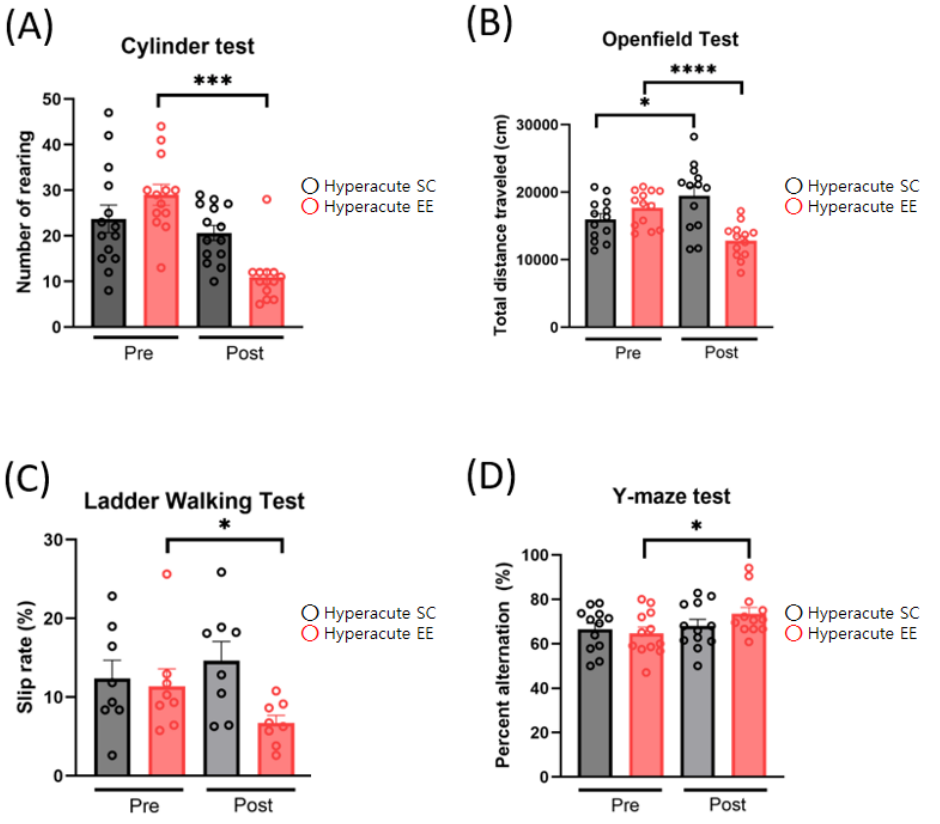

Figure 3. Hyperacute exposure to 2 weeks of EE improves neurobehavioral function after HI brain injury (SC, n = 35; EE, n = 35). (A) In the cylinder test, the total rearing was significantly reduced in the EE group compared with the SC group (***$p < 0.001$, independent t-test) (B) In the open field test, the total distance traveled between the EE (n = 35) and SC control mice (n = 35) showed a significant difference (****$p < 0.0001$, independent t-test). (C) In the ladder rung walking test, the percentage of slips relative to the total number of steps by the hemiplegic forelimbs decreased significantly in the enriched mice, compared with the SC controls (*$p < 0.05$, independent t-test). (D) In the Y-maze test, the percentage of alternations improved significantly in the EE group compared with the control group (*$p < 0.05$, independent t-test). Data represent mean ± SEM values.

D. Hyperacute exposure to EE downregulates genes associated with cell death and regulation of apoptosis

To investigate the therapeutic mechanisms of hyperacute exposure to EE, we performed RNA-seq for transcriptome analysis to explore DEGs in the cortex and hippocampus of mouse brain. We selected DEGs based on greater than 2-fold change from all identified genes. The selected 1,691 DEGs (220 upregulated and 1,471 downregulated) in cortex and 2,942 DEGs (866 upregulated and 2,076 downregulated) in hippocampus in enriched mice were identified.

The downregulated genes in the brain of enriched mice in hyperacute phase were categorized according to biological process, molecular function, cellular components and pathway using the DAVID software program. Based on the GO analysis, the top 10 biological processes of the downregulated genes in cerebral cortex and hippocampus were related to “cellular process” (GO:0009987), “biological regulation” (GO:0065007), “regulation of biological process” (GO:0050789), “response to stimulus” (GO:0050896), “regulation of cellular process” (GO:0050794), and “metabolic process” (GO:0008152). Genes, which were commonly downregulated in cerebral cortex and hippocampus, were also highly involved in “cell death” (GO:0008219), “apoptotic process” (GO:0006915), “regulation of cell death” (GO:0010941), “regulation of programmed cell death” (GO: 0043067), and “regulation of apoptotic process” (GO: 0042981). Further, in KEGG pathway, the highlighted cluster in the downregulated genes significantly expressed the overall theme for apoptosis (Table 1, 2, Figure 4, 5). Table 3 demonstrates apoptosis-related genes, which were generally downregulated in the cerebral cortex and hippocampus of mice in the hyperacute EE group.

Table 1. Kyoto Encyclopedia of Genes and Genomes (KEGG) pathways revealed significantly downregulated genes in the cerebral cortex of mouse brain enriched in hyperacute phase using Database for Annotation, Visualization and Integrated Discovery (DAVID) software

Term	Count	P-Value	Genes	Fold Enrichment
mmu05150: Staphylococcus aureus infection	28	0.000	*C3AR1, C3, MASP2, ITGB2, C1QC, C1RA, CFH, C2, ICAM1, C5AR1, C4B, CFB, HC, FCGR4, H2-DMB1, H2-AB1, FCGR1, H2-DMB2, FCGR3, C1QA, C1QB, H2-OA, FCGR2B, H2-OB, H2-EB1, H2-AA, C1S1, PTAFR*	7.623
mmu04145: Phagosome	45	0.000	*RAB7B, C3, TLR2, H2-D1, TLR4, ITGB2, TLR6, C1RA, TAP2, TAP1, THBS1, PLA2R1, THBS2, THBS4, TCIRG1, H2-Q2, MRC1, H2-K1, H2-M3, NCF2, NCF1, NCF4, MRC2, FCGR4, H2-DMB1, COLEC12, H2-AB1, CTSS, H2-Q7, FCGR1, H2-Q8, H2-DMB2, FCGR3, CYBA, CTSL, CD36, FCGR2B, H2-OA, ITGA5, H2-BL, H2-EB1, H2-OB, H2-AA, CLEC7A, CD14*	3.582
mmu04610: Complement and coagulation cascades	26	0.000	*C3AR1, A2M, C5AR1, C4B, C3, CFB, MASP2, HC, F13A1, F9, SERPING1, C1QC, PLAUR, C1QA, C1RA, C1QB, THBD, F5, SERPINF2, CD46, CFH, TFPI, C2, C1S1, PROS1, PLAU*	4.657
mmu04512: ECM-receptor interaction	27	0.000	*COL3A1, ITGA10, HMMR, CHAD, CD44, GP1BB, COL6A5, ITGB7, COL27A1, COL6A2, COL6A1, THBS1, THBS2, THBS4, FN1, SPP1, COL4A3, COL5A2, COL4A6, COL5A1, COL4A5, LAMA1, CD36, ITGA5, ITGA8, COL1A2, COL1A1*	4.177
mmu04060: Cytokine-cytokine receptor interaction	48	0.000	*CCL3, CXCL5, CSF2RB2, TNFRSF25, OSMR, CSF1, LEPR, CCR1, IL21R, CCL9, PF4, IL15, IL7R, TNFRSF4, CCL6, CXCL10, CCL24, TNFRSF11B, CCL22, TNFRSF1B, CLCF1, CXCR4, IL10RB, IL10RA, CSF2RB, CSF3R, IL2RG, FAS, IL13RA1, LTB, PRL, CSF2RA, IL1A, IFNLR1, IL2RB, TGFBR2, EDA2R, CCL19, CCR9, CCL12, TNFSF10, TNFRSF10B, TNFSF13B, CCR5, CXCL16, CCR2, GM21586, IL3RA*	2.700
mmu05323: Rheumatoid arthritis	25	0.000	*TCIRG1, ICAM1, CCL3, CXCL5, CSF1, TLR2, ACP5, H2-DMB1, TLR4, ITGB2, H2-AB1, IL15, H2-DMB2,*	4.150

			CCL12, CTSL, CD86, CTSK, TNFSF13B, CD80, H2-OA, H2-EB1, H2-OB, H2-AA, LTB, IL1A	
mmu05152: Tuberculosis	38	0.000	*C3, TLR1, TLR2, TLR4, ITGB2, TLR6, CD74, TLR9, NOD2, CYP27B1, ITGAX, IL10RB, IL10RA, CASP8, FCER1G, LBP, PLA2R1, IL1A, TCIRG1, MRC1, CARD9, MRC2, FCGR4, H2-DMB1, MALT1, H2-AB1, CTSS, FCGR1, H2-DMB2, FCGR3, H2-OA, FCGR2B, H2-OB, H2-EB1, H2-AA, CTSD, CLEC7A, CD14*	2.939
mmu05168: Herpes simplex infection	40	0.000	*TRAF1, IFIH1, C3, TLR2, H2-D1, IL15, OAS2, CD74, TLR9, CFP, TAP2, TAP1, CASP8, FAS, PILRA, H2-Q2, H2-K1, CDK1, SP100, H2-M3, SOCS3, HC, H2-DMB1, H2-AB1, H2-Q7, H2-Q8, CDK2, H2-DMB2, CCL12, IKBKE, IFIT1, H2-OA, IRF7, H2-BL, H2-EB1, H2-OB, OAS1B, H2-AA, OAS1A, EIF2AK2*	2.618
mmu04974: Protein digestion and absorption	24	0.000	*COL18A1, COL4A3, COL3A1, COL15A1, COL5A2, SLC6A19, COL4A6, COL5A1, KCNJ13, SLC7A7, COL4A5, COL9A1, SLC1A5, COL14A1, COL7A1, COL6A5, COL27A1, KCNK5, COL6A2, COL1A2, COL12A1, COL6A1, COL1A1, COL10A1*	3.712
mmu05140: Leishmaniasis	20	0.000	*PTPN6, NCF2, NCF1, C3, NCF4, FCGR4, TLR2, H2-DMB1, TLR4, ITGB2, H2-AB1, FCGR1, H2-DMB2, FCGR3, CYBA, H2-OA, H2-OB, H2-EB1, H2-AA, IL1A*	4.254
mmu05332: Graft-versus-host disease	18	0.000	*H2-Q2, H2-K1, H2-M3, H2-D1, H2-DMB1, H2-AB1, H2-Q7, H2-Q8, H2-DMB2, CD86, CD80, H2-OA, H2-BL, H2-OB, H2-EB1, H2-AA, FAS, IL1A*	4.712
mmu05133: Pertussis	21	0.000	*CXCL5, C4B, HC, C3, TLR4, ITGB2, SERPING1, NLRP3, C1QC, C1QA, C1RA, C1QB, ITGA5, IRF8, TICAM2, PYCARD, C2, C1S1, CASP1, CD14, IL1A*	3.863
mmu04151: PI3K-Akt signaling pathway	54	0.000	*FGF7, OSMR, PGF, TLR2, LPAR4, TLR4, CHAD, CSF3R, PIK3AP1, PDGFD, MYB, PRL, MYC, FGF3, PIK3CG, CDK6, CDK2, LPAR5, LPAR6, COL1A2, GNB3, COL1A1, YWHAZ, CSF1, COL3A1, ITGA10, IL7R, COL6A5, ITGB7, COL27A1, COL6A2, COL6A1, IL2RG, THBS1, THBS2, PIK3R1, SPP1, FN1, THBS4, COL4A3, IL2RB, FLT4, IGF1, HGF, COL5A2, COL4A6, COL5A1, COL4A5, LAMA1, GNGT2, ITGA5, ITGA8, IL3RA, GH*	2.094
mmu04612: Antigen processing and presentation	22	0.000	*H2-Q2, H2-K1, H2-M3, H2-D1, IFI30, H2-DMB1, H2-AB1, CTSS, H2-Q7, CD74, H2-Q8, H2-DMB2, B2M, CTSL, H2-OA, TAP2, H2-BL, TAP1, H2-OB, H2-EB1, H2-AA, PSME2B*	3.652

mmu05416: Viral myocarditis	21	0.000	*H2-Q2, H2-K1, ICAM1, H2-M3, H2-D1, H2-DMB1, ITGB2, H2-AB1, MYH6, H2-Q7, H2-Q8, H2-DMB2, CD86, RAC2, H2-OA, CD80, H2-BL, CASP8, H2-OB, H2-EB1, H2-AA*	3.618
mmu04672:Intestinal immune network for IgA production	15	0.000	*ICOSL, H2-DMB1, H2-AB1, IL15, H2-DMB2, CCR9, CD86, TNFSF13B, CD80, H2-OA, CXCR4, ITGB7, H2-OB, H2-EB1, H2-AA*	4.862
mmu04940: Type I diabetes mellitus	18	0.000	*H2-Q2, H2-K1, H2-M3, H2-D1, H2-DMB1, H2-AB1, H2-Q7, H2-Q8, H2-DMB2, CD86, CD80, H2-OA, H2-BL, H2-OB, H2-EB1, H2-AA, FAS, IL1A*	3.952
mmu05330: Allograft rejection	17	0.000	*H2-Q2, H2-K1, H2-M3, H2-D1, H2-DMB1, H2-AB1, H2-Q7, H2-Q8, H2-DMB2, CD86, H2-OA, CD80, H2-BL, H2-OB, H2-EB1, H2-AA, FAS*	4.132
mmu05164:Influenza A	32	0.000	*IFIH1, RSAD2, TLR4, OAS2, IL33, TLR7, CXCL10, PYCARD, FAS, CASP1, MX2, PIK3R1, IL1A, PIK3CG, ICAM1, SOCS3, H2-DMB1, H2-AB1, NLRP3, H2-DMB2, CCL12, IKBKE, TNFSF10, TNFRSF10B, H2-OA, IRF7, H2-EB1, H2-OB, OAS1B, H2-AA, OAS1A, EIF2AK2*	2.547
mmu04380: Osteoclast differentiation	26	0.000	*CSF1, SPI1, ACP5, NFKB2, BTK, TNFRSF11B, LILRA5, IL1A, PIK3R1, TYROBP, PIK3CG, NCF2, NCF1, SOCS3, NCF4, TGFBR2, FCGR4, FCGR1, FCGR3, PIRB, CYBA, CYBB, CTSK, FCGR2B, TREM2, LCP2*	2.809
mmu05322: Systemic lupus erythematosus	28	0.000	*C3, HIST2H3C1, C1QC, C1RA, HIST1H2BN, GRIN2B, C2, HIST1H4H, HIST1H2BC, C4B, HC, HIST1H2BH, FCGR4, H2-DMB1, H2-AB1, FCGR1, H2-DMB2, TRIM21, C1QA, C1QB, CD86, CD80, H2-OA, H2-OB, H2-EB1, H2-AA, HIST1H3D, C1S1*	2.593
mmu04640: Hematopoietic cell lineage	20	0.000	*CSF1, ANPEP, CD1D1, IL7R, CD24A, FCGR1, CD9, CD37, CD36, CD44, ITGA5, GP1BB, CD33, H2-EB1, CSF3R, CD22, CSF2RA, CD14, IL3RA, IL1A*	3.203
mmu05320: Autoimmune thyroid disease	18	0.000	*H2-Q2, H2-K1, H2-M3, H2-D1, H2-DMB1, H2-AB1, H2-Q7, H2-Q8, H2-DMB2, CD86, CD80, H2-OA, H2-BL, H2-OB, H2-EB1, H2-AA, FAS, TSHR*	3.451
mmu04620: Toll-like receptor	22	0.000	*PIK3CG, CCL3, TLR1, TLR2, TLR4, TLR6, TLR7, TLR9, CXCL10, IKBKE, CD86, CTSK, IRF5, CD80, IRF7, CASP8, MAP3K8, TICAM2, LBP, CD14, PIK3R1, SPP1*	2.965

signaling pathway				
mmu05162: Measles	26	0.000	*IFIH1, TLR2, TLR4, OAS2, TLR7, TLR9, CD46, IL2RG, MSN, FAS, MX2, PIK3R1, IL1A, PIK3CG, IL2RB, CDK6, CDK2, IKBKE, DOK1, TNFSF10, TNFRSF10B, FCGR2B, IRF7, OAS1B, OAS1A, EIF2AK2*	2.602
mmu04510: Focal adhesion	34	0.000	*PGF, COL3A1, ITGA10, CHAD, RAC2, COL6A5, COL27A1, ITGB7, COL6A2, COL6A1, PDGFD, THBS1, THBS2, PIK3R1, THBS4, SPP1, FN1, PIK3CG, COL4A3, FLT4, IGF1, HGF, FLNC, BIRC3, COL5A2, VAV1, COL4A6, COL5A1, COL4A5, LAMA1, ITGA5, ITGA8, COL1A2, COL1A1*	2.236
mmu05166: HTLV-I infection	41	0.000	*WNT16, TSPO, SPI1, H2-D1, ITGB2, CHEK2, IL15, NFKB2, POLE2, CDKN2B, IL2RG, NFATC4, MYB, MYC, PIK3R1, H2-Q2, H2-K1, PIK3CG, ZFP36, ICAM1, IL2RB, EGR2, H2-M3, TGFBR2, H2-DMB1, H2-AB1, FZD5, H2-Q7, H2-Q8, FZD7, H2-DMB2, WNT2B, MSX1, ATF3, H2-OA, H2-BL, H2-EB1, H2-OB, BUB1B, H2-AA, WNT11*	2.022
mmu04514: Cell adhesion molecules (CAMs)	27	0.000	*CLDN3, H2-D1, ITGB2, CDH1, ITGB7, CD22, H2-K1, H2-Q2, ICAM1, PTPRC, ICOSL, H2-M3, H2-DMB1, H2-AB1, H2-Q7, H2-DMB2, H2-Q8, CD86, CD80, H2-OA, ITGA8, H2-BL, H2-OB, H2-EB1, CLDN1, CLDN2, H2-AA*	2.269
mmu05205: Proteoglycans in cancer	31	0.000	*WNT16, LUM, TLR2, TLR4, DCN, MMP2, CD44, HPSE, MSN, FAS, THBS1, MYC, PIK3R1, TWIST1, FN1, PIK3CG, PTPN6, IGF1, HGF, FLNC, CD63, FZD5, FZD7, WNT2B, PLAUR, CTSL, ITGA5, COL1A2, WNT11, COL1A1, PLAU*	2.079
mmu05321:Inflammatory bowel disease (IBD)	14	0.000	*IL21R, TLR2, H2-DMB1, RORC, TLR4, H2-AB1, H2-DMB2, NOD2, H2-OA, H2-OB, H2-EB1, H2-AA, IL2RG, IL1A*	3.230
mmu05146: Amoebiasis	21	0.000	*PIK3CG, COL4A3, GNA14, RAB7B, COL3A1, TLR2, TLR4, ITGB2, COL5A2, COL4A6, COL5A1, COL4A5, LAMA1, SERPINB6B, COL27A1, COL1A2, HSPB1, COL1A1, CD14, PIK3R1, FN1*	2.443
mmu05202: Transcriptional misregulation in cancer	26	0.000	*SLC45A3, TRAF1, CEBPA, NFKBIZ, IL2RB, WNT16, LMO2, TGFBR2, SPI1, IGF1, HIST2H3C1, FCGR1, MLF1, HHEX, CD86, FLI1, BCL2A1B, LYL1, ITGB7, SIX1, HIST1H3D, RUNX1, HPGD, MYC, PLAU, CD14*	2.145

mmu05144: Malaria	12	0.000	*CCL12, ICAM1, GYPC, CD36, TLR2, TLR4, ITGB2, HGF, THBS1, THBS2, THBS4, TLR9*	3.403
mmu04621: NOD-like receptor signaling pathway	13	0.000	*CARD9, NLRP1B, NLRP3, BIRC3, NAIP6, CCL12, NOD2, NAIP2, CASP8, NAIP5, PYCARD, NAIP1, CASP1*	3.105
mmu05134: Legionellosis	13	0.000	*NAIP6, NAIP2, C3, NAIP5, CASP8, PYCARD, TLR2, TLR4, ITGB2, NFKB2, NAIP1, CASP1, CD14*	3.105
mmu04630:Jak-STAT signaling pathway	23	0.000	*PIK3CG, PTPN6, IL2RB, OSMR, CSF2RB2, SOCS3, LEPR, IL21R, IL15, IL7R, IL10RB, IL10RA, CSF2RB, CSF3R, IL2RG, IL13RA1, MYC, PRL, CSF2RA, GH, IL3RA, PIK3R1, IFNLR1*	2.159
mmu04668: TNF signaling pathway	19	0.000	*PIK3CG, TRAF1, ICAM1, SOCS3, CSF1, IL15, GM5431, MMP14, BIRC3, CXCL10, CCL12, NOD2, TNFRSF1B, CASP8, MAP3K8, BCL3, MLKL, FAS, PIK3R1*	2.373
mmu05310: Asthma	8	0.001	*H2-OA, H2-EB1, H2-OB, H2-DMB1, FCER1G, H2-AA, H2-AB1, H2-DMB2*	4.537
mmu04662: B cell receptor signaling pathway	14	0.002	*PIK3CG, PTPN6, MALT1, CD72, VAV1, BTK, CARD11, FCGR2B, RAC2, DAPP1, CD22, PIK3AP1, CD79B, PIK3R1*	2.722
mmu04064: NF-kappa B signaling pathway	17	0.002	*TRAF1, ICAM1, CCL19, TLR4, MALT1, NFKB2, BIRC3, BTK, LAT, CARD11, TNFSF13B, BCL2A1B, TICAM2, LBP, LTB, CD14, PLAU*	2.386
mmu04666: Fc gamma R-mediated phagocytosis	15	0.003	*PIK3CG, PTPRC, NCF1, LIMK1, HCK, ASAP3, VAV1, FCGR1, WAS, ARPC1B, LAT, DOCK2, FCGR2B, RAC2, PIK3R1*	2.431
mmu04115:p53 signaling pathway	13	0.003	*STEAP3, CDK1, IGF1, CDK6, CHEK2, CDK2, GTSE1, CCNB1, RRM2, CASP8, FAS, PERP, THBS1*	2.641
mmu04142: Lysosome	19	0.003	*TCIRG1, NAGLU, CTSZ, LITAF, AP1G2, GUSB, HEXB, ACP5, CTSS, CD63, DNASE2A, SLC11A1, CTSL, CTSK, CD68, LAPTM5, CTSD, CTSC, CTSH*	2.120
mmu04650: Natural killer cell mediated cytotoxicity	17	0.004	*PIK3CG, PTPN6, ICAM1, FCGR4, ITGB2, VAV1, CD48, LAT, TNFSF10, TNFRSF10B, RAC2, FCER1G, FAS, PIK3R1, SH3BP2, TYROBP, LCP2*	2.204

mmu04670: Leukocyte transendothelial migration	18	0.005	*PIK3CG, ICAM1, NCF2, CLDN3, NCF1, NCF4, ITGB2, VAV1, MMP2, CTNNA3, CYBA, RAC2, CXCR4, CLDN1, CLDN2, MSN, PIK3R1, RHOH*	2.076
mmu05222: Small cell lung cancer	14	0.008	*TRAF1, PIK3CG, COL4A3, CDK6, BIRC3, COL4A6, CDK2, COL4A5, LAMA1, CDKN2B, CKS2, MYC, PIK3R1, FN1*	2.269
mmu05142: Chagas disease (American trypanosomiasis)	16	0.008	*PIK3CG, GNA14, CCL3, C3, TGFBR2, TLR2, TLR4, TLR6, C1QC, TLR9, C1QA, C1QB, CCL12, CASP8, FAS, PIK3R1*	2.115
mmu05340: Primary immunodeficiency	8	0.010	*DCLRE1C, PTPRC, TAP2, TAP1, IL2RG, IL7R, ADA, BTK*	3.203
mmu04210: Apoptosis	11	0.011	*PIK3CG, TNFSF10, TNFRSF10B, CSF2RB2, CASP12, CASP8, CSF2RB, FAS, BIRC3, PIK3R1, IL3RA*	2.496
mmu04664: Fc epsilon RI signaling pathway	10	0.059	*PIK3CG, LAT, PLA2G4A, RAC2, FCER1G, PLA2G4C, VAV1, PIK3R1, LCP2, BTK*	2.002
mmu05020: Prion diseases	6	0.090	*C1QA, C1QB, HC, CASP12, C1QC, IL1A*	2.475

Table 2. Kyoto Encyclopedia of Genes and Genomes (KEGG) pathways revealed significantly downregulated genes in the hippocampus of mouse brains enriched in hyperacute phase using Database for Annotation, Visualization and Integrated Discovery (DAVID) software

Term	Count	P-Value	Genes	Fold Enrichment
mmu04512:ECM-receptor interaction	46	2.40E-17	*COL3A1, ITGA11, ITGB5, ITGA10, VTN, ITGB3, SDC4, ITGB1, HMMR, LAMB2, CD44, COL6A6, COL6A5, COL6A4, COL27A1, ITGB7, COL6A3, COL6A2, COL6A1, TNN, THBS1, COL11A2, THBS2, THBS4, SPP1, FN1, ITGA1, HSPG2, COL5A3, COL5A2, COL4A6, COL5A1, COL4A5, VWF, LAMA1, SDC1, LAMA4, CD36, LAMA3, ITGA6, ITGA5, LAMC3, COL1A2, LAMC2, COL1A1, ITGA2B*	3.851
mmu05150:Staphylococcus aureus infection	30	1.86E-13	*C3AR1, ITGAL, C3, ITGB2, C1QC, ITGAM, C1RA, CFH, C2, ICAM1, C5AR1, C4B, CFB, HC, FCGR4, H2-DMB1, H2-AB1, FCGR1, H2-DMB2, FCGR3, C1QA, C1QB, FCGR2B, H2-OA, H2-EB1, H2-OB, H2-AA, C1S1, H2-DMA, PTAFR*	4.420
mmu04060:Cytokine-cytokine receptor interaction	73	2.02E-11	*OSMR, LEPR, IL21R, GDF5, TNFSF13, TNFSF12, IL15, CXCL12, TGFB1, CXCL10, IL17RB, TNFRSF11B, TNFRSF11A, CLCF1, CXCR4, CSF2RB, CSF3R, FAS, IL13RA1, PRL, LTB, IFNGR1, IL1A, LTA, LTBR, TNFRSF17, IL11RA1, TNFRSF14, EDAR, CCR9, IFNAR2, TNFRSF9, IL20RB, CCR5, GM13308, CCR2, CX3CR1, IL1R2, CCL3, CXCL5, CSF2RB2, TNFRSF12A, CSF1, CCR1, IL4RA, CCL9, PF4, IL7R, CCL28, CCL6, TNFRSF1A, CCL22, TNFRSF1B, IL17B, IL10RB, IL10RA, IL2RG, CSF1R, GM2506, AMHR2, IL2RB, TGFBR1, TGFBR2, GM20878, TNFRSF13C, CCL19, IL6RA, CCL12, TNFSF10, PRLR, CXCL16, BMP7, IL3RA*	2.222
mmu05140:Leishmaniasis	31	1.00E-10	*PTGS2, C3, TLR2, NFKBIA, TLR4, ITGB2, ITGB1, TGFB1, ITGAM, IRAK4, MYD88, NOS2, IFNGR1, IL1A, PTPN6, NCF2, NCF1, NCF4, FCGR4, H2-DMB1, H2-AB1, STAT1, FCGR1,*	3.568

			H2-DMB2, FCGR3, CYBA, H2-OA, H2-OB, H2-EB1, H2-AA, H2-DMA	
mmu04080 :Neuroactive ligand-receptor interaction	80	1.02E-10	*TSPO, ADORA3, TACR3, LEPR, TACR1, GLRA2, F2RL1, LPAR3, VIPR2, SCTR, S1PR2, EDNRA, S1PR3, HTR1B, A630033H20RIK, S1PR4, CHRNA7, GLP2R, HTR1D, CHRNA1, PRL, HTR1F, CHRNA3, C5AR1, RXFP1, PTGER4, RXFP3, HTR4, GRM1, GRM5, SSTR4, GABRR2, CRHR2, CHRM5, ADRB2, CHRM2, AGTR1A, LPAR6, PTGDR, GPR50, TSHR, PTAFR, C3AR1, CYSLTR1, ADORA2A, DRD5, NPY2R, OPRK1, TRHR, OXTR, HCRTR2, APLNR, HCRTR1, ADRB3, P2RY6, CNR1, P2RY2, CNR2, MAS1, ADRA2B, GABRQ, GABRE, PTH2R, GABRA5, PTGFR, NPY5R, P2RX4, P2RY13, P2RX7, GPR35, P2RX6, PRLR, GRIA2, GRIA1, P2RX3, P2RY14, CHRNB1, NMBR, HTR2C, HTR2A*	2.068
mmu04380 :Osteoclast differentiation	46	2.05E-10	*CSF1, PPARG, SPI1, ACP5, NFKBIA, ITGB3, NFKB2, TGFB1, BTK, TNFRSF1A, TNFRSF11B, TNFRSF11A, LILRA5, PIK3R5, MAP2K7, IFNGR1, IL1A, CSF1R, TYROBP, TEC, BLNK, NFATC1, SYK, PIK3CG, NCF2, SOCS3, NCF1, TGFBR1, NCF4, TGFBR2, FCGR4, STAT1, FCGR1, FCGR3, PIRB, IRF9, IFNAR2, CYBA, CTSK, CYBB, FCGR2B, LCK, PLCG2, MAP3K14, TREM2, LCP2*	2.689
mmu04145 :Phagosome	55	6.48E-10	*TUBB2A, H2-D1, TLR2, TLR4, TLR6, CANX, C1RA, TUBB6, H2-K1, DYNC1I1, NCF2, NCF1, NCF4, H2-DMB1, COLEC12, CTSS, H2-DMB2, CTSL, CD36, H2-OA, H2-T9, H2-OB, H2-AA, RAB7B, C3, ITGB5, ITGB2, ITGB3, ITGB1, ITGAM, ATP6V0E, TAP2, TAP1, THBS1, PLA2R1, THBS2, THBS4, TCIRG1, MRC1, H2-M3, MRC2, FCGR4, H2-AB1, H2-Q7, FCGR1, FCGR3, CYBA, FCGR2B, ITGA5, H2-EB1, H2-T23, CLEC7A, H2-T24, H2-DMA, CD14*	2.369
mmu04064 :NF-kappa B signaling pathway	38	1.02E-09	*TRAF1, PTGS2, NFKBIA, TLR4, NFKB2, CXCL12, BTK, IRAK4, VCAM1, TNFRSF1A, MYD88, TNFRSF11A, ZAP70, TICAM2, LBP, LTB, TRAF5, LTA, BLNK, SYK, ICAM1, LTBR, LYN, LY96, TNFRSF13C, CCL19, TRIM25, BIRC3, DDX58, CARD11, LAT, BCL2A1B, RIPK1, LCK, PLCG2, MAP3K14, PLAU, CD14*	2.886

mmu04510 :Focal adhesion	60	8.42E -09	*TLN1, VTN, SHC1, COL11A2, PIK3CG, PARVG, PRKCG, ACTN2, ACTN3, FLNC, VASP, CCND3, LAMC3, COL1A2, LAMC2, COL1A1, ITGA2B, CAV1, ERBB2, COL3A1, ITGA11, ITGB5, ITGA10, ITGB3, ITGB1, MYL9, LAMB2, RAC2, COL6A6, COL6A5, COL6A4, ITGB7, COL27A1, COL6A3, COL6A2, COL6A1, PIK3R5, TNN, THBS1, THBS2, FN1, SPP1, THBS4, ITGA1, IGF1, MYL12A, HGF, BIRC3, COL5A3, VAV1, COL5A2, COL4A6, COL5A1, COL4A5, LAMA1, VWF, LAMA4, LAMA3, ITGA6, ITGA5*	2.135
mmu04974 :Protein digestion and absorption	34	1.35E -08	*SLC16A10, COL3A1, ELN, SLC7A7, SLC1A5, COL9A1, COL9A2, COL6A6, COL7A1, COL6A5, COL6A4, COL27A1, COL6A3, KCNK5, COL6A2, COL12A1, COL6A1, COL11A2, DPP4, COL10A1, COL18A1, COL13A1, SLC3A1, COL5A3, COL5A2, COL4A6, COL5A1, XPNPEP2, COL4A5, KCNN4, COL14A1, COL1A2, PRCP, COL1A1*	2.846
mmu04672 :Intestinal immune network for IgA production	22	1.57E -08	*LTBR, TNFRSF13C, TNFRSF17, H2-DMB1, TNFSF13, H2-AB1, IL15, CCL28, CXCL12, TGFB1, H2-DMB2, CCR9, CD86, CD80, H2-OA, CXCR4, ITGB7, H2-EB1, H2-OB, H2-AA, MAP3K14, H2-DMA*	3.859
mmu05145 :Toxoplasmosis	37	4.57E -08	*LDLR, TLR2, NFKBIA, TLR4, ITGB1, TGFB1, IRAK4, HSPA1L, TNFRSF1A, IGTP, MYD88, LAMB2, IL10RB, IL10RA, CASP8, NOS2, IFNGR1, IRGM1, LY96, H2-DMB1, H2-AB1, BIRC3, STAT1, H2-DMB2, LAMA1, LAMA4, LAMA3, H2-OA, ITGA6, CCR5, LAMC3, H2-EB1, H2-OB, H2-AA, LAMC2, ALOX5, H2-DMA*	2.596
mmu05152 :Tuberculosis	52	4.87E -08	*TLR1, TLR2, TLR4, TLR6, TGFB1, TLR9, MYD88, CASP8, NOS2, LBP, IL1A, IFNGR1, SYK, H2-DMB1, FADD, CTSS, H2-DMB2, H2-OA, H2-OB, CTSD, H2-AA, KSR1, C3, ITGB2, CD74, ITGAM, IRAK4, VDR, TNFRSF1A, ITGAX, IL10RB, IL10RA, FCER1G, PLA2R1, MRC1, TCIRG1, CEBPB, CARD9, MRC2, SPHK1, FCGR4, H2-AB1, STAT1, FCGR1, FCGR3, LSP1, FCGR2B, H2-EB1, CLEC7A, APAF1, H2-DMA, CD14*	2.177

mmu05323 :Rheumatoid arthritis	31	1.17E-07	*ITGAL, CCL3, CXCL5, CSF1, TLR2, ACP5, TNFSF13, TLR4, ITGB2, IL15, CXCL12, TGFB1, ATP6V0E, TNFRSF11A, LTB, IL1A, TCIRG1, ICAM1, H2-DMB1, H2-AB1, H2-DMB2, CTSL, CCL12, CD86, CTSK, CD80, H2-OA, H2-OB, H2-EB1, H2-AA, H2-DMA*	2.785
mmu05133 :Pertussis	29	1.36E-07	*CXCL5, C3, TLR4, ITGB2, C1QC, ITGB1, ITGAM, IRAK4, C1RA, MYD88, CASP7, PYCARD, TICAM2, C2, NOS2, CASP1, IL1A, LY96, C4B, HC, SERPING1, NLRP3, C1QA, C1QB, ITGA5, IRF8, IRF1, C1S1, CD14*	2.887
mmu05146 :Amoebiasis	38	3.16E-07	*IL1R2, GNA14, GNA15, RAB7B, COL3A1, TLR2, TLR4, ITGB2, SERPINB1B, TGFB1, ITGAM, LAMB2, COL27A1, PIK3R5, NOS2, COL11A2, PLCB2, FN1, PIK3CG, ACTN2, PRKCG, ACTN3, COL5A3, COL5A2, COL4A6, COL5A1, COL4A5, LAMA1, LAMA4, LAMA3, SERPINB6A, LAMC3, SERPINB6B, COL1A2, HSPB1, LAMC2, COL1A1, CD14*	2.393
mmu05321 :Inflammatory bowel disease (IBD)	24	9.65E-07	*MAF, IL4RA, IL21R, TLR2, RORC, H2-DMB1, TLR4, H2-AB1, TLR5, RORA, STAT1, TGFB1, H2-DMB2, STAT6, STAT4, H2-OA, H2-EB1, H2-OB, H2-AA, IL2RG, H2-DMA, IFNGR1, IL1A, NFATC1*	2.997
mmu04610 :Complement and coagulation cascades	28	9.90E-07	*C3AR1, C7, A2M, C3, F13A1, C1QC, C1RA, SERPINE1, CFH, C2, C5AR1, HC, CFB, C4B, F9, SERPING1, PLAUR, C1QA, VWF, C1QB, THBD, F5, SERPINF2, TFPI, SERPIND1, C1S1, PROS1, PLAU*	2.714
mmu04640 :Hematopoietic cell lineage	30	1.04E-06	*IL1R2, CSF1, IL4RA, ANPEP, KIT, ITGB3, IL7R, CD24A, ITGAM, CD9, CD44, CSF3R, CD22, CD4, IL1A, CSF1R, ITGA1, IL11RA1, FCGR1, IL6RA, CD37, CD36, ITGA6, ITGA5, CD34, CD33, H2-EB1, CD14, IL3RA, ITGA2B*	2.600
mmu04612 :Antigen processing and presentation	29	1.57E-06	*LGMN, H2-D1, IFI30, CANX, CD74, TAPBP, B2M, HSPA1L, TAP2, TAP1, CD4, H2-K1, H2-M3, H2-DMB1, H2-AB1, CTSS, H2-Q7, H2-DMB2, CTSL, H2-OA, H2-T9, PSME2, H2-OB, H2-EB1, H2-AA, H2-T23, H2-T24, CTSB, H2-DMA*	2.605
mmu04620 :Toll-like receptor	33	1.89E-06	*CCL3, TLR1, TLR2, TLR3, NFKBIA, TLR4, TLR5, TLR6, TLR7, TLR9, CXCL10, IRAK4, MYD88, MAP3K8, CASP8, TICAM2, PIK3R5, LBP,*	2.407

signaling pathway			*MAP2K7, SPP1, PIK3CG, LY96, FADD, STAT1, IKBKE, IFNAR2, CD86, CTSK, IRF5, CD80, RIPK1, IRF7, CD14*	
mmu05162 :Measles	39	6.52E -06	*MAVS, IFIH1, RAB9B, TACR1, STAT5A, TLR2, NFKBIA, TLR4, OAS2, TLR7, TLR9, IRAK4, HSPA1L, MYD88, IL2RG, PIK3R5, MSN, FAS, MX2, IFNGR1, IL1A, PIK3CG, IL2RB, CDK6, STAT1, SLAMF1, CDK2, DDX58, IRF9, IFNAR2, IKBKE, DOK1, TNFSF10, CCND3, FCGR2B, IRF7, OAS1B, OAS1A, JAK3*	2.113
mmu04668 :TNF signaling pathway	33	1.15E -05	*TRAF1, PTGS2, CSF1, MMP9, NFKBIA, GM5431, IL15, CXCL10, VCAM1, TNFRSF1A, TNFRSF1B, CASP7, CASP8, MAP3K8, BCL3, MLKL, PIK3R5, CREB3L3, FAS, TRAF5, MAP2K7, LTA, PIK3CG, ICAM1, CEBPB, SOCS3, IFI47, FADD, MMP14, BIRC3, CCL12, RIPK1, MAP3K14*	2.230
mmu04670 :Leukocyte transendothelial migration	34	2.56E -05	*ITGAL, CLDN3, MMP9, ITGB2, CXCL12, MMP2, ITGB1, ITGAM, CLDN15, MYL9, VCAM1, RAC2, PTK2B, CXCR4, PIK3R5, MSN, RHOH, PIK3CG, F11R, ICAM1, NCF2, NCF1, NCF4, ACTN2, PRKCG, MYL12A, ACTN3, VAV1, VASP, CLDN24, PTPN11, CYBA, PLCG2, CLDN2*	2.123
mmu04666 :Fc gamma R-mediated phagocytosis	26	7.98E -05	*WASF3, WASF1, ASAP3, AMPH, DOCK2, RAC2, GSN, PIK3R5, INPP5D, SYK, PIK3CG, PTPRC, LYN, NCF1, HCK, SPHK1, PRKCG, WAS, PRKCD, VAV1, FCGR1, VASP, LAT, ARPC1B, FCGR2B, PLCG2*	2.280
mmu05222 :Small cell lung cancer	26	7.98E -05	*TRAF1, E2F2, PTGS2, NFKBIA, ITGB1, LAMB2, CDKN2B, PIK3R5, NOS2, MYC, TRAF5, FN1, PIK3CG, CDK6, BIRC3, COL4A6, CDK2, COL4A5, LAMA1, LAMA4, LAMA3, ITGA6, LAMC3, LAMC2, APAF1, ITGA2B*	2.280
mmu04662 :B cell receptor signaling pathway	23	8.63E -05	*PIK3CG, PTPN6, LYN, NFKBIE, NFKBIA, CD72, VAV1, BTK, CARD11, DAPP1, RAC2, RASGRP3, FCGR2B, PLCG2, CD22, PIK3AP1, CD79B, PIK3R5, CD79A, INPP5D, SYK, BLNK, NFATC1*	2.421
mmu05332 :Graft-versus-host disease	19	9.34E -05	*H2-K1, H2-M3, H2-D1, H2-DMB1, H2-AB1, H2-Q7, H2-DMB2, CD86, CD80, H2-OA, H2-T9, H2-OB, H2-EB1, H2-AA, H2-T23, H2-T24, FAS, H2-DMA, IL1A*	2.692

mmu05144 :Malaria	18	1.05E -04	*ITGAL, GYPC, ICAM1, TLR2, TLR4, ITGB2, HGF, TGFB1, TLR9, VCAM1, CCL12, SDC1, MYD88, CD36, HBB-B2, THBS1, THBS2, THBS4*	2.763
mmu04115 :p53 signaling pathway	22	1.30E -04	*STEAP3, CDK1, IGF1, CDK6, CHEK2, PMAIP1, CDK2, CCNB1, CDKN1A, CCNB2, CCND3, RRM2, CD82, CASP8, SERPINE1, APAF1, MDM4, FAS, THBS1, PERP, GADD45B, GADD45A*	2.419
mmu05416 :Viral myocarditis	24	2.19E -04	*H2-K1, ITGAL, ICAM1, CAV1, H2-M3, H2-D1, H2-DMB1, ITGB2, H2-AB1, MYH6, H2-Q7, H2-DMB2, CD86, RAC2, CD80, H2-OA, H2-T9, CASP8, H2-OB, H2-EB1, H2-AA, H2-T23, H2-T24, H2-DMA*	2.238
mmu04350 :TGF-beta signaling pathway	25	2.70E -04	*LTBP1, GDF5, DCN, TGFB1, ACVR1C, CDKN2B, LEFTY2, THBS1, MYC, BMP4, AMHR2, TGFBR1, SMAD6, RBL1, TGFBR2, LEFTY1, ID1, TGIF1, TGIF2, ID3, BMP7, BAMBI, BMP8B, BMP5, BMP6*	2.167
mmu05134 :Legionellosis	19	3.49E -04	*C3, TLR2, NFKBIA, TLR4, ITGB2, NFKB2, TLR5, ITGAM, HSPA1L, NAIP6, MYD88, NAIP2, CASP7, CASP8, NAIP5, PYCARD, APAF1, CASP1, CD14*	2.456
mmu04940 :Type I diabetes mellitus	20	3.71E -04	*H2-K1, H2-M3, H2-D1, H2-DMB1, H2-AB1, H2-Q7, H2-DMB2, CD86, CD80, H2-OA, H2-T9, H2-OB, H2-EB1, H2-AA, H2-T23, H2-T24, FAS, H2-DMA, IL1A, LTA*	2.376
mmu05142 :Chagas disease (American trypanosomiasis)	28	4.32E -04	*GNA14, CCL3, GNA15, C3, TLR2, NFKBIA, TLR4, TLR6, C1QC, TGFB1, TLR9, IRAK4, TNFRSF1A, MYD88, SERPINE1, CASP8, PIK3R5, FAS, NOS2, PLCB2, IFNGR1, PIK3CG, TGFBR1, TGFBR2, FADD, C1QA, C1QB, CCL12*	2.003
mmu05330 :Allograft rejection	18	8.40E -04	*H2-K1, H2-M3, H2-D1, H2-DMB1, H2-AB1, H2-Q7, H2-DMB2, CD86, H2-OA, CD80, H2-T9, H2-OB, H2-EB1, H2-AA, H2-T23, H2-T24, FAS, H2-DMA*	2.368
mmu05340 :Primary immunodeficiency	13	0.001	*PTPRC, TNFRSF13C, IL7R, ADA, BTK, TAP2, TAP1, LCK, ZAP70, IL2RG, CD4, CD79A, BLNK*	2.817
mmu04210 :Apoptosis	18	0.002	*PIK3CG, CSF2RB2, NFKBIA, FADD, BIRC3, TNFRSF1A, CASP6, TNFSF10, RIPK1, CASP7,*	2.210

			CASP12, CASP8, CSF2RB, PIK3R5, APAF1, FAS, MAP3K14, IL3RA	
mmu05412 :Arrhythmogenic right ventricular cardiomyopathy (ARVC)	19	0.003	*CACNG8, CACNG6, ITGA11, ITGA1, ITGB5, ITGA10, ITGB3, CACNB4, ITGB1, CACNA2D2, TCF7L2, TCF7L1, DES, ITGA6, ITGA5, PKP2, ITGB7, DSP, ITGA2B*	2.089
mmu05310 :Asthma	10	0.003	*H2-OA, EPX, H2-EB1, H2-OB, H2-DMB1, FCER1G, H2-AA, H2-AB1, H2-DMA, H2-DMB2*	3.070
mmu04978 :Mineral absorption	12	0.012	*VDR, TRPM6, FTL1, TRPM7, HMOX1, MT2, CYBRD1, MT1, HEPH, SLC39A4, STEAP2, STEAP1*	2.267
mmu05143 :African trypanosomiasis	11	0.015	*VCAM1, ICAM1, LAMA4, MYD88, F2RL1, PRKCG, HBB-B2, FAS, IDO1, PLCB2, TLR9*	2.315
mmu00603 :Glycosphingolipid biosynthesis - globo series	6	0.042	*A4GALT, GBGT1, HEXA, HEXB, NAGA, FUT2*	2.947

Table 3. List of genes commonly downregulated in the regions of mouse brain in hyperacute phase after HI brain injury

Gene symbol	Description	Fold change in cerebral cortex	Fold change in hippocampus
PIK3CG	phosphoinositide-3-kinase, catalytic, gamma polypeptide	-2.49	-4.12
TNFSF10	Tumor necrosis factor superfamily, member 10	-3.069	-3.46
CSF2RB2	Colony stimulating factor 2 receptor, beta 2, low-affinity (granulocyte-macrophage)	-12.81	-12.73
CASP12	caspase 12	-12.65	-10.24
CASP8	caspase 8	-2.45	-6.24
CSF2RB	Colony stimulating factor 2receptor, beta, low-affinity (granulocyte-macrophage)	-6.94	-20.10
FAS	Fas (TNF receptor superfamily member 6)	-3.79	-4.06
BIRC3	baculoviral IAP repeat-containing 3	-2.36	-4.35
IL3RA	Interleukin 3receptor, alpha chain	-2.81	-4.10

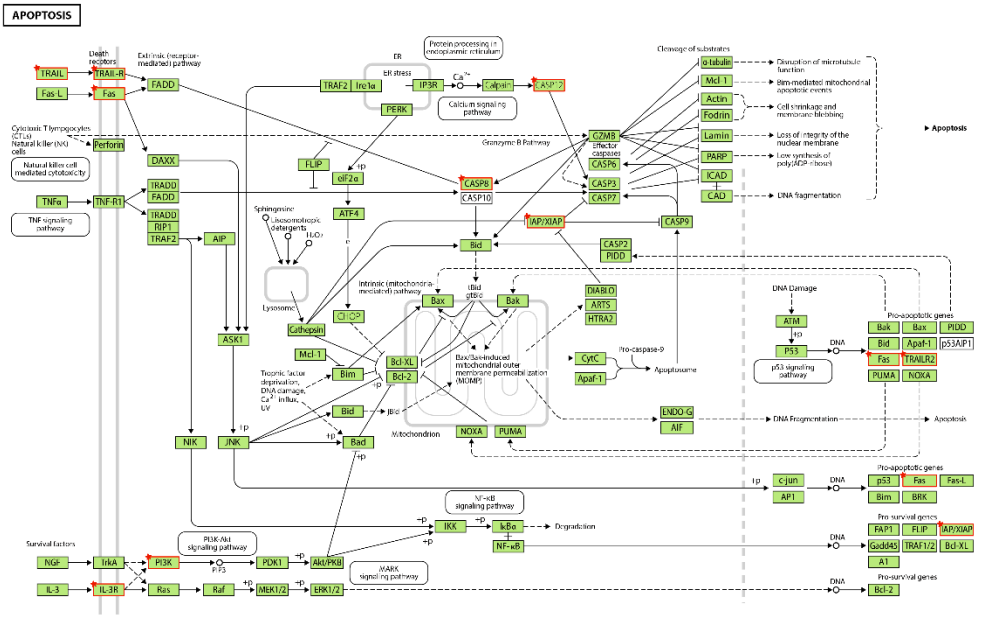

Figure 4. The main KEGG pathway was significantly downregulated in cerebral cortex following hyperacute exposure to EE. Red means that the protein is downregulated by hyperacute exposure to EE. The network diagram was sourced from KEGG database.

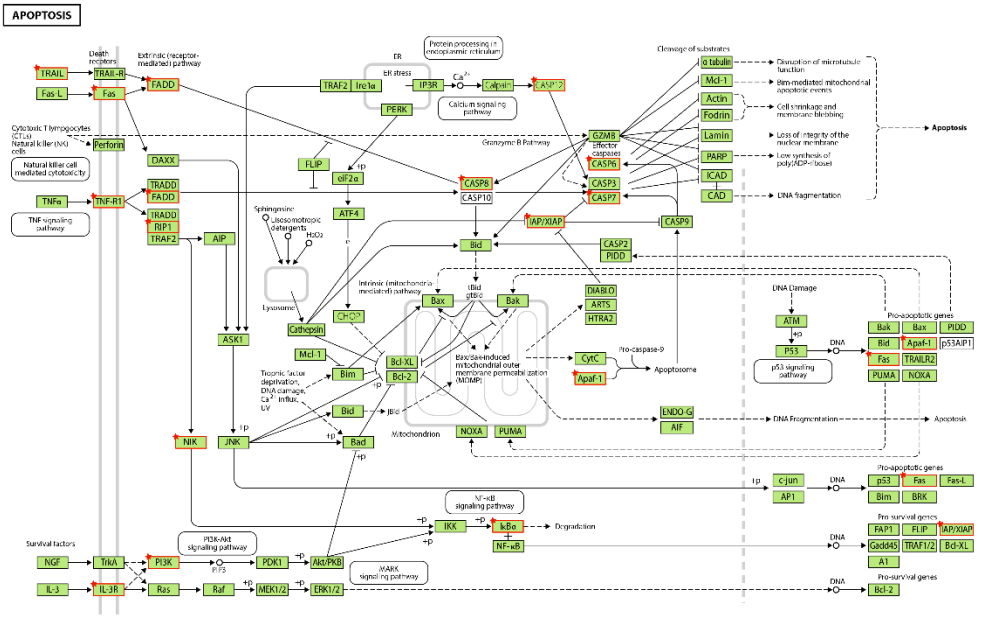

Figure 5. The main KEGG pathway significantly downregulated in hippocampus by hyperacute exposure to EE. Red means that the protein is downregulated by hyperacute exposure to EE. The diagram used in the network analysis was derived from KEGG database.

E. Hyperacute exposure to EE alters the expression of genes associated with extrinsic apoptosis in cerebral cortex and hippocampus

We analyzed the role of hyperacute exposure to EE after HI brain injury in the inhibition of the extrinsic pathway of apoptosis. The GO and KEGG pathway enrichment analyses indicated significant downregulation of *TNFSF10, FAS*, and *CASP8* in the cortex and hippocampus of the enriched mice.

The protein encoded by *TNFSF10* is a cytokine belonging to the TNF ligand family and preferentially induces apoptosis in transformed and tumor cells. This protein binds to several members of TNF receptor superfamily including TNFRSF10A/TRAILR1, TNFRSF10B/TRAILR2, TNFRSF10C/TRAILR3, and TNFRSF10D/TRAILR4, triggering the activation of MAPK8/JNK, caspase-8, and caspase-3. *FAS* encodes the protein belonging to the TNF receptor superfamily. It has been shown to play a central role in the physiological regulation of programmed cell death, pathogenesis of various malignancies and diseases of the immune system. The interaction of this death receptor with its ligand facilitates the formation of DISC including FADD and caspase-8. FADD is an adapter molecule that recruits caspase-8 to the activated receptor. The resulting DISC undergoes caspase-8 proteolytic cleavage, which initiates the subsequent cascade of apoptosis mediated by the caspases. *Caspase-8* encodes a member of the caspase family. Sequential activation of caspases plays a central role in the execution phase of cellular apoptosis. The protein mediates programmed cell death induced by Fas and various apoptotic stimuli. The N-terminal FADD-like death effector domain of this protein suggests possible interaction with Fas-interacting protein FADD.

F. Hyperacute exposure to EE contributes to neuroprotection by decreasing the expression of both extrinsic and intrinsic apoptosis-related proteins in cerebral cortex and hippocampus

Western blot analysis was conducted to further validate the effects of downregulating Fas/FasL-mediated apoptosis and to evaluate the connection between intrinsic apoptosis pathways in cerebral cortex and hippocampus. The western blots representing FAS,

FADD, cleaved caspase-8, total caspase-8, cleaved caspase-3, total caspase-3, Bax, Bcl-2 and β-Actin in the hyperacute EE and SC groups are shown in Figure 6. The expression of FAS, FADD, and Bax was significantly suppressed, while the Bcl-2 expression was significantly increased, and the ratios of cleaved caspase-8 to total caspase-8, Bax to Bcl-2, and cleaved caspase-3 to total caspase-3 were significantly decreased in the cerebral cortex and the hippocampus of the hyperacute EE group compared with the control group (Figure 6).

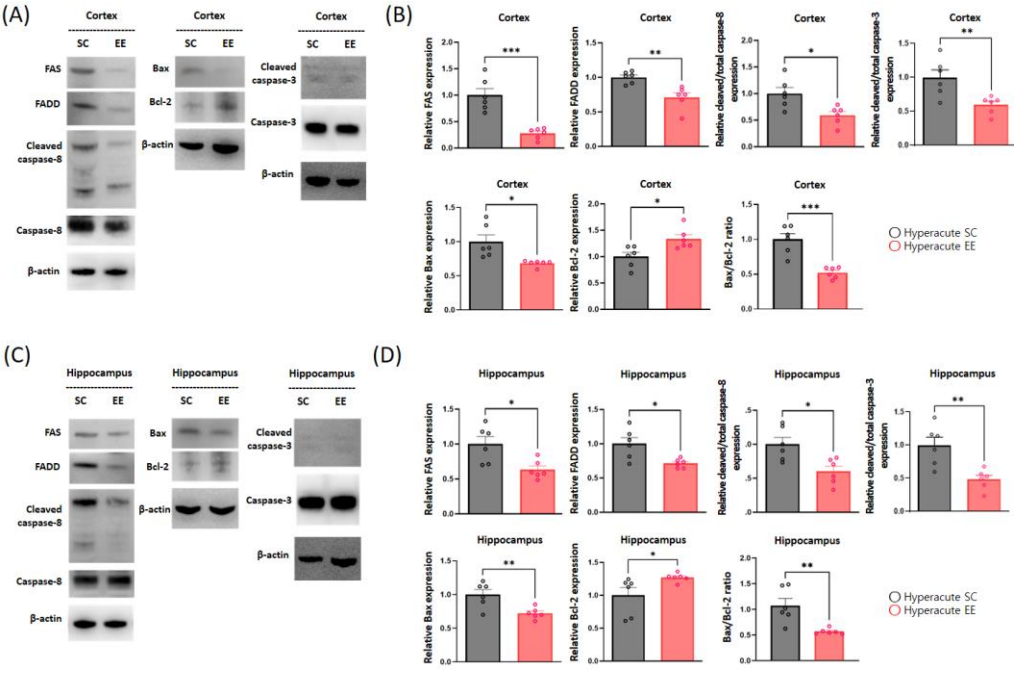

Figure 6. Expression of extrinsic and intrinsic apoptosis-related proteins in cerebral cortex and hippocampus (SC, n = 6; EE, n = 6). The levels of FAS, FADD, and Bax, and the ratios of cleaved caspase-8 to total caspase-8, Bax to Bcl-2, and cleaved caspase-3 to total caspase-3 were significantly decreased, whereas the expression of Bcl-2 was significantly increased in the cerebral cortex of mice exposed to very early EE compared with SC mice (A, B) (***$p < 0.001$, **$p < 0.01$, *$p < 0.05$, *$p < 0.05$, ***$p < 0.001$, **$p < 0.01$, *$p < 0.05$, respectively). The expression of FAS, FADD, and Bax, and the ratios of cleaved caspase-8 to total caspase-8, Bax to Bcl-2, and cleaved caspase-3 to total caspase-3 decreased significantly, while the expression of Bcl-2 was increased significantly in the hippocampus of mice under very early EE compared with SC mice (C, D) (*$p < 0.05$, *$p < 0.05$, **$p < 0.01$, *$p < 0.05$, **$p < 0.01$, **$p < 0.01$, *$p < 0.05$, respectively)

G. Hyperacute exposure to EE reduces infarct volume

The effect of hyperacute exposure to EE on infarct volume was observed at 2 weeks after the mice were exposed to either EE or SC. The infarct volumes were notably decreased in the hyperacute EE group when compared with the control group ($P < 0.05$, Figures 7 (a) and 8 (b)).

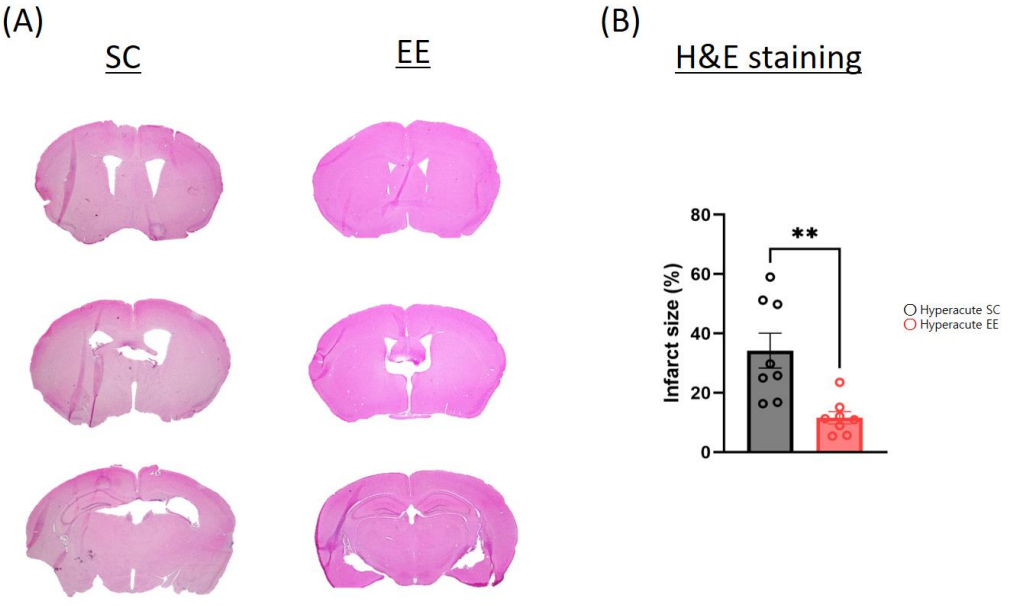

Figure 7. Hyperacute EE protects brain tissue and reduces infarct volume from HI brain injury in mice (SC, n = 8; EE, n = 8). (a) Representative photographs of brain slices of mice showing infarct volume assessed 2 weeks after hyperacute exposure to either EE or SC. (b) The infarct volumes as percentages of contralateral hemisphere were analyzed via independent t-test (**$p < 0.01$).

H. Hyperacute exposure to EE decreases DNA fragmentation of brain cells and neuronal apoptosis in cerebral cortex and hippocampus

To evaluate the neuroprotective effect of hyperacute exposure to EE, immunohistochemical analysis of the cortex and hippocampus was performed by

quantifying the TUNEL-positive (TUNEL+) cells (n = 8 each) and the endogenous expression of MAP-2-positive (MAP-2+) and FADD-positive (FADD+) neurons (n = 4 each) (Figure 8, 9). The results of TUNEL assay showed that DNA fragmentation in brain cells was significantly decreased in the cortex and hippocampus of mice exposed to hyperacute EE compared with SC mice. In the double immunostaining for MAP-2 and FADD, the fluorescence intensity of apoptotic neurons was significantly decreased in the cortex and hippocampus of EE mice compared with SC mice.

Therefore, our results established that hyperacute EE experienced after HI brain injury induces downregulation of Fas/FasL-mediated apoptosis and protects neuronal cells in the cerebral cortex and hippocampus from apoptosis, facilitates recovery from motor and cognitive function, and ameliorates anxiety and hyperactivity.

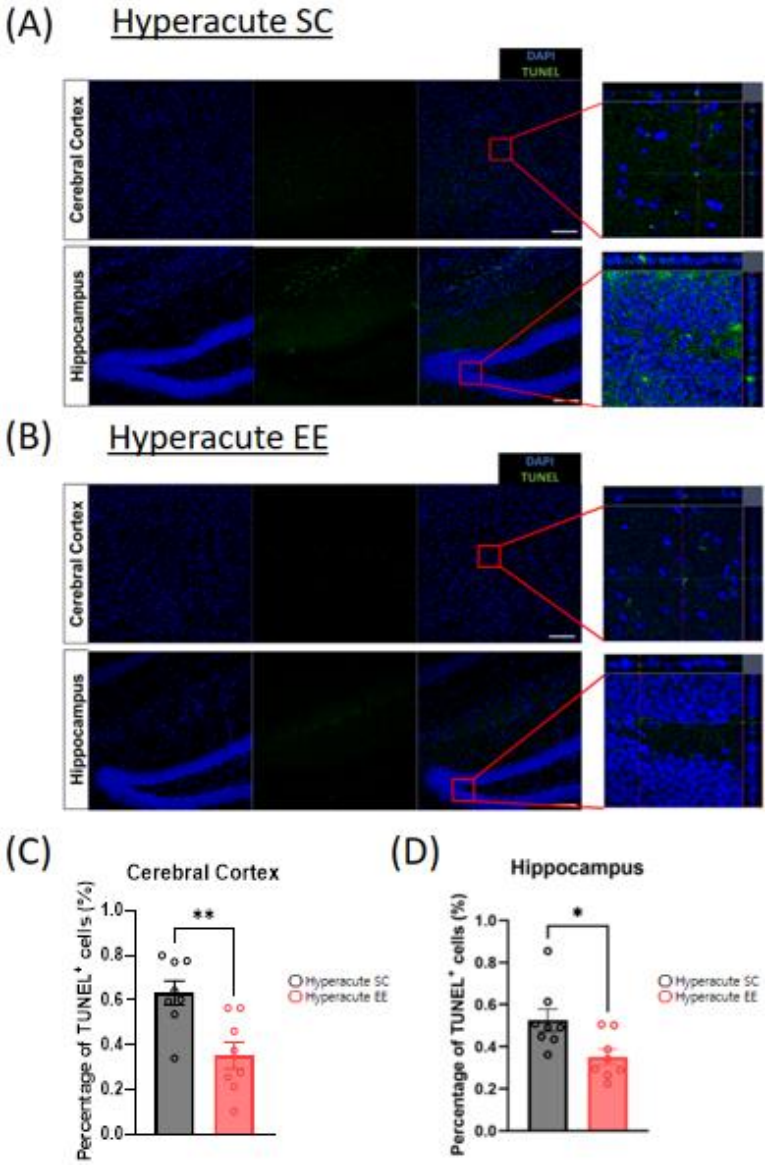

Figure 8. Hyperacute exposure to EE decreases TUNEL staining in cerebral cortex and hippocampus after HI brain injury (SC, n = 8; EE, n = 8). TUNEL+ cells are indicated in green (A, B). TUNEL+ cells in in both cerebral cortex and hippocampus of hyperacute EE mice were significantly decreased compared with control mice (C, D). Values are means ± SEM. An asterisk indicates significant difference (*$p < 0.05$ and **$p < 0.01$ by Mann–Whitney U-test). Scale bars represent 100 μm.

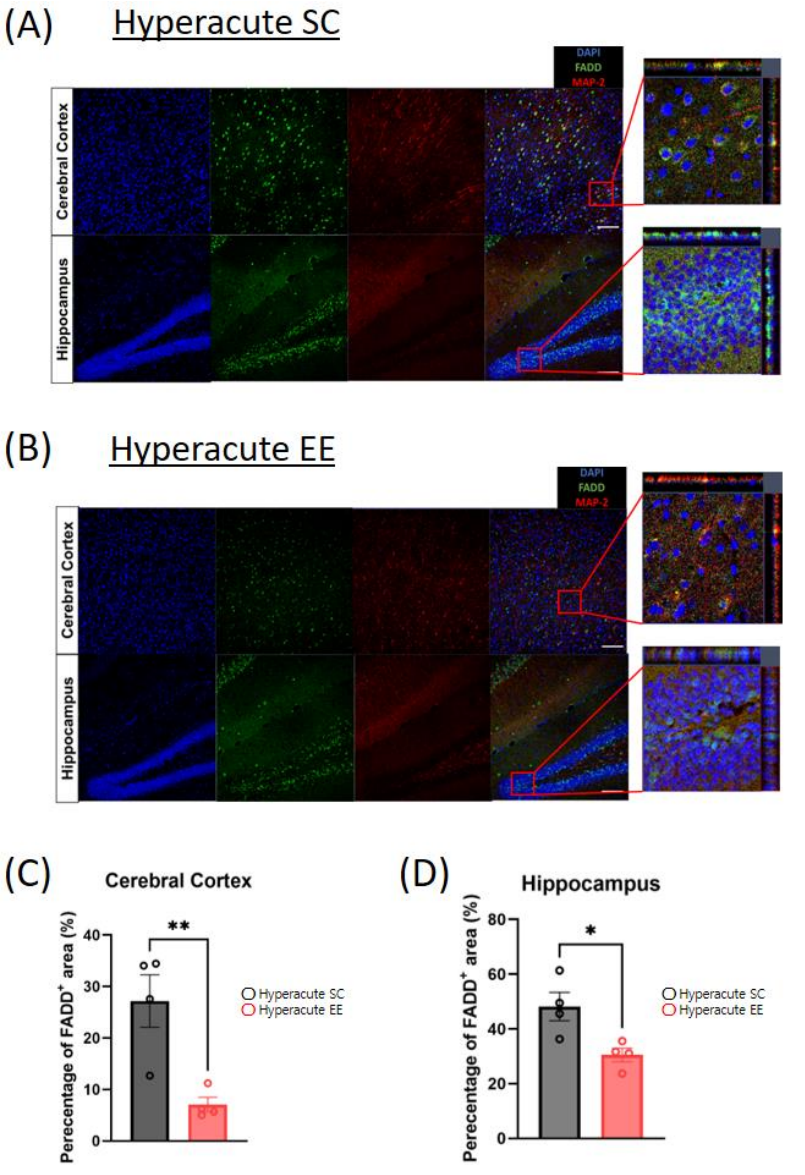

Figure 9. Hyperacute exposure to EE decreases double immunostaining of FADD and MAP-2 in cerebral cortex and hippocampus after HI brain injury (SC, n = 4; EE, n = 4). FADD+ neurons are indicated in green (A, B). FADD+ cells in in both cortex and hippocampus of hyperacute EE mice decreased significantly compared with control mice (C, D). Values are means ± SEM. An asterisk indicates significant difference (*$p <$ 0.05 and **$p < 0.01$ by Mann–Whitney U-test). Scale bars represent 100 μm.

2. Delayed EE model

We investigated behavioral, histological, and molecular changes induced by delayed exposure to EE in adult mice sustaining HI brain injury to compare the effects on Fas/FasL-mediated apoptosis, neuronal survival, and neurobehavioral outcomes with those induced in hyperacute EE model. The experimental design of the delayed EE mouse model is described in Figure 1D.

A. Delayed exposure to EE decreases anxiety and hyperactivity in cylinder and open field tests

In the cylinder test, the rearing count in the delayed EE group was significantly reduced compared with the SC controls (Figure 10A). During the 25 min of open field test, the total distance traveled decreased significantly in the delayed EE group compared with the SC controls (Figure 10B), suggesting that delayed EE exposure aleviates anxiety and hyperactivity after HI brain injury.

B. Delayed exposure to EE improves fine motor function in ladder walking test

Delayed exposure to EE group showed a significant reduction in the percentage of total slips among the total steps with both forelimbs (Figure 10C). It suggests that delayed exposure to EE improves asymmetrical use of forelimbs and fine motor function.

C. Delayed exposure to EE improves cognitive function in Y-maze test

Cognitive performance was significantly enhanced in EE mice based on the increase in the number of alterations in Y-maze test (Figure 10D).

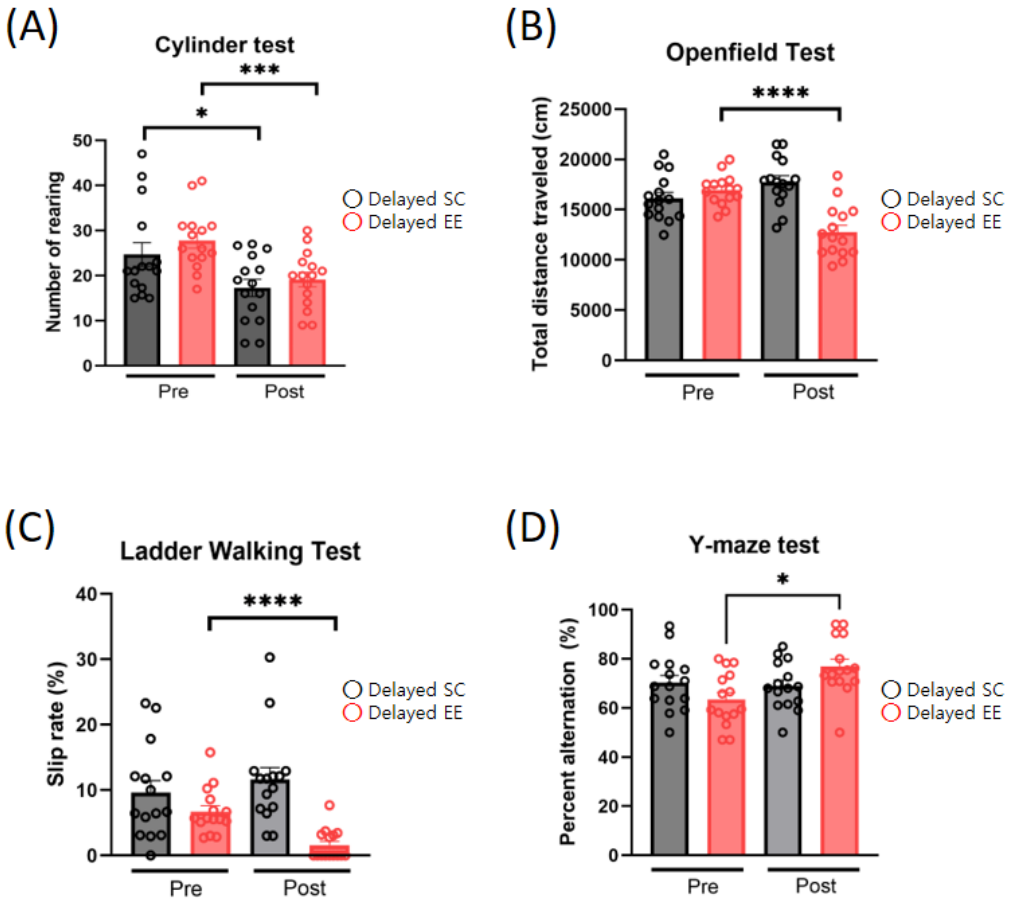

Figure 10. Delayed exposure to EE improves neurobehavioral function after HI brain injury (SC, n = 20; EE, n = 20). (A) In the cylinder test, the total rearing number was significantly reduced in the EE group compared with the SC group (***$p < 0.001$) (B) In the open field test, there was a significant difference in the total distance travelled between the EE and SC control mice (****$p < 0.0001$) The behavioral analysis showed that delayed exposure to EE after HI improves anxiety and hyperactivity. (C) In the ladder walking test, the percentage of slips relative to the total number of steps by the hemiplegic forelimbs were significantly decreased in the enriched mice, compared with the SC controls. (****$p < 0.0001$) (D) In the Y-maze test, the percentage of alternation was significantly improved in the EE group compared with the control group (*$p <$ 0.05). Data are mean ± SEM, based on independent t-test

D. Delayed exposure to EE does not suppress the expression of apoptosis execution-related proteins in cerebral cortex and hippocampus

In the delayed EE group, the relative protein expression of FAS, FADD, and the ratio of cleaved caspase-8 to total caspase-8 were significantly decreased compared with the control group in cortex. However, the expression of FAS and the ratio of cleaved caspase-8 to total caspase-8 in the hippocampus did not show a significant difference compared with the control group (Figure 11 B, D). The ratio of cleaved caspase-3 to total caspase-3 in in cortex did not differ significantly between the delayed EE and SC groups; however, it increased significantly in the delayed EE group compared with the control group. The relative protein expression of Bax and the ratio of Bax to Bcl-2 in intrinsic apoptosis increased significantly, while the expression of Bcl-2 in cortex was significantly decreased in the delayed EE group compared with the SC group. The expression of Bax, Bcl-2, and the ratio of Bax to Bcl-2 in hippocampus did not differ significantly between the delayed EE and SC groups (Figures 11 B, D).

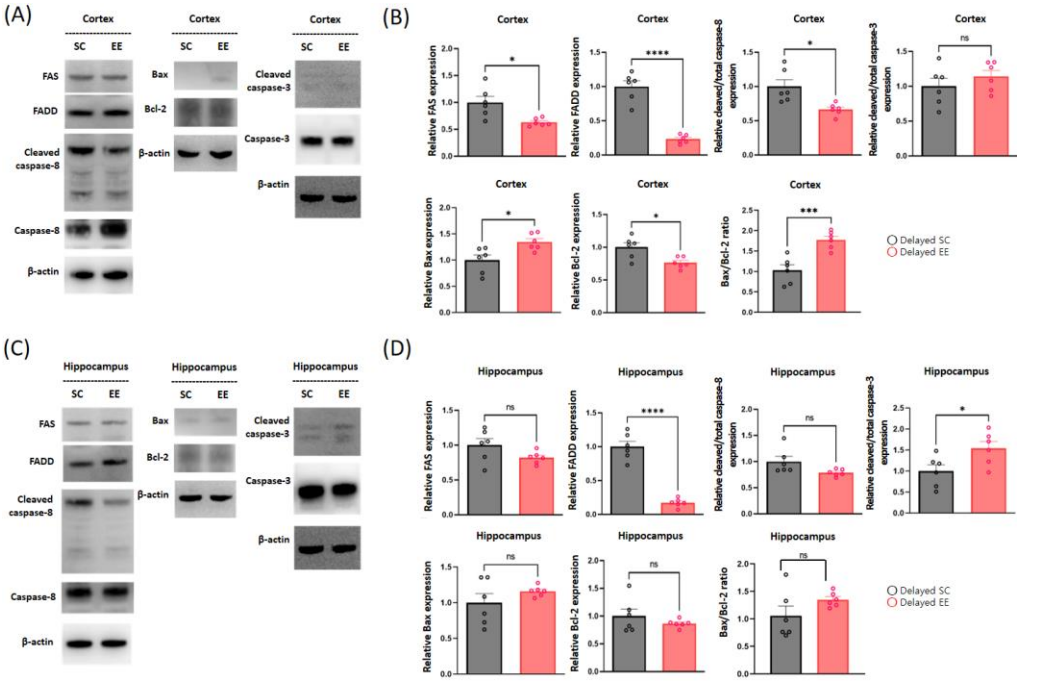

Figure 11. Effects of delayed exposure to EE or SC on the expression of extrinsic and intrinsic apoptosis-related proteins in cerebral cortex and hippocampus after HI brain injury (SC, n = 6; EE, n = 6). The relative expression of FAS, FADD, and Bcl-2 proteins in the cerebral cortex and the ratio of cleaved caspase-8 to total caspase-8 were significantly decreased, while Bax and the ratio of Bax to Bcl-2 increased significantly in mice with delayed EE compared with SC mice (*$p < 0.05$, ****$p < 0.0001$, *$p < 0.05$, *$p < 0.05$, *$p < 0.05$, ***$p < 0.001$, respectively). The ratio of cleaved caspase-3 to total caspase-3 in the cerebral cortex did not differ significantly between the two groups in cerebral cortex ($p = 0.300$). The relative protein expression of FADD in hippocampus was significantly decreased and the ratio of cleaved caspase-3 to caspase-3 was significantly increased in the delayed EE mice compared with SC mice (****$p < 0.0001$, *$p < 0.05$, respectively)

E. Delayed exposure to EE reduces infarct volume

The effect of delayed exposure to EE on infarct volume was observed at 2 weeks after the mice were exposed to either EE or SC 3 days after the HI brain injury. The infarct volumes were significantly decreased in the delayed EE group when compared with the control group (P < 0:05, Figures 12 A and 12 B).

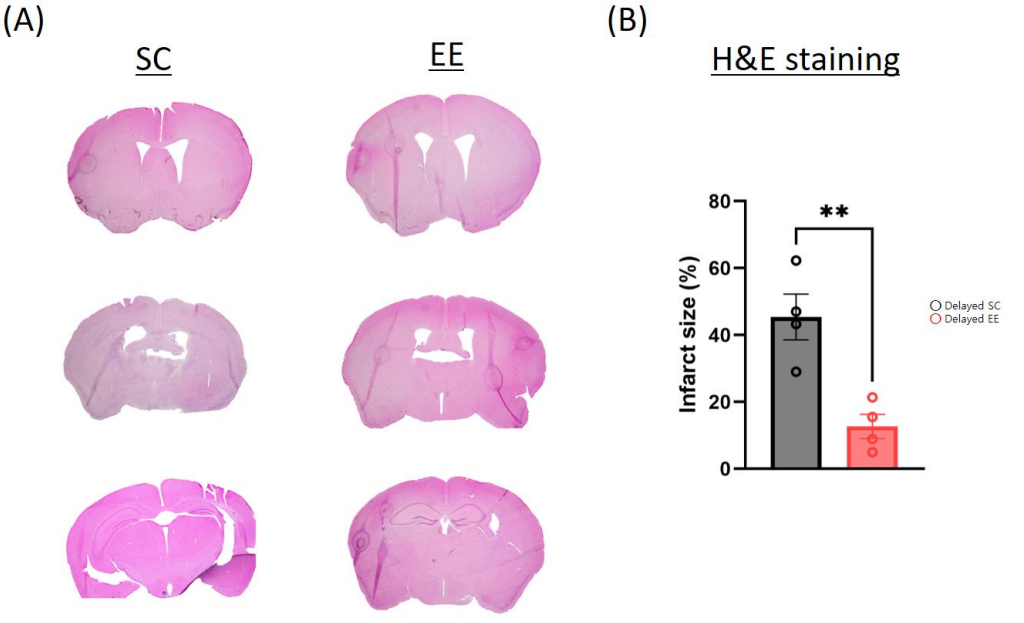

Figure 12. Delayed EE treatment protects brain tissue and reduces infarct volume in mice with HI brain injury (SC, n = 4; EE, n = 4). (a) Representative photographs of brain slices showing infarct volume assessed 2 weeks after exposure to either EE or SC 3 days after HI brain injury. (b) The infarct volumes as percentages of the contralateral hemisphere based on independent t-test (**$p < 0.01$).

F. Delayed exposure to EE decreases DNA fragmentation of brain cells but not neuronal apoptosis in cerebral cortex and hippocampus.

To evaluate the neuroprotective effects of delayed exposure to EE,

immunohistochemical analysis was performed in the cortex and hippocampus by measuring the number of TUNEL-positive (TUNEL+) cells and quantifying the endogenous expression of MAP-2-positive (MAP-2+) and FADD-positive (FADD+) neurons (Figure 13, 14). Results of TUNEL assay showed a significant decrease in DNA fragmentation of brain cells in the cortex and hippocampus of mice exposed to delayed EE compared with SC mice. The fluorescence intensity of apoptotic neurons in the cortex and hippocampus subjected to double immunostaining for MAP-2 and FADD did not show a significant difference between mice exposed to delayed EE and SC mice.

Therefore, delayed EE experienced after HI brain injury protects against overall DNA fragmentation of brain cells in the cerebral cortex and hippocampus but does not prevent Fas/FasL pathway-related neuronal apoptosis.

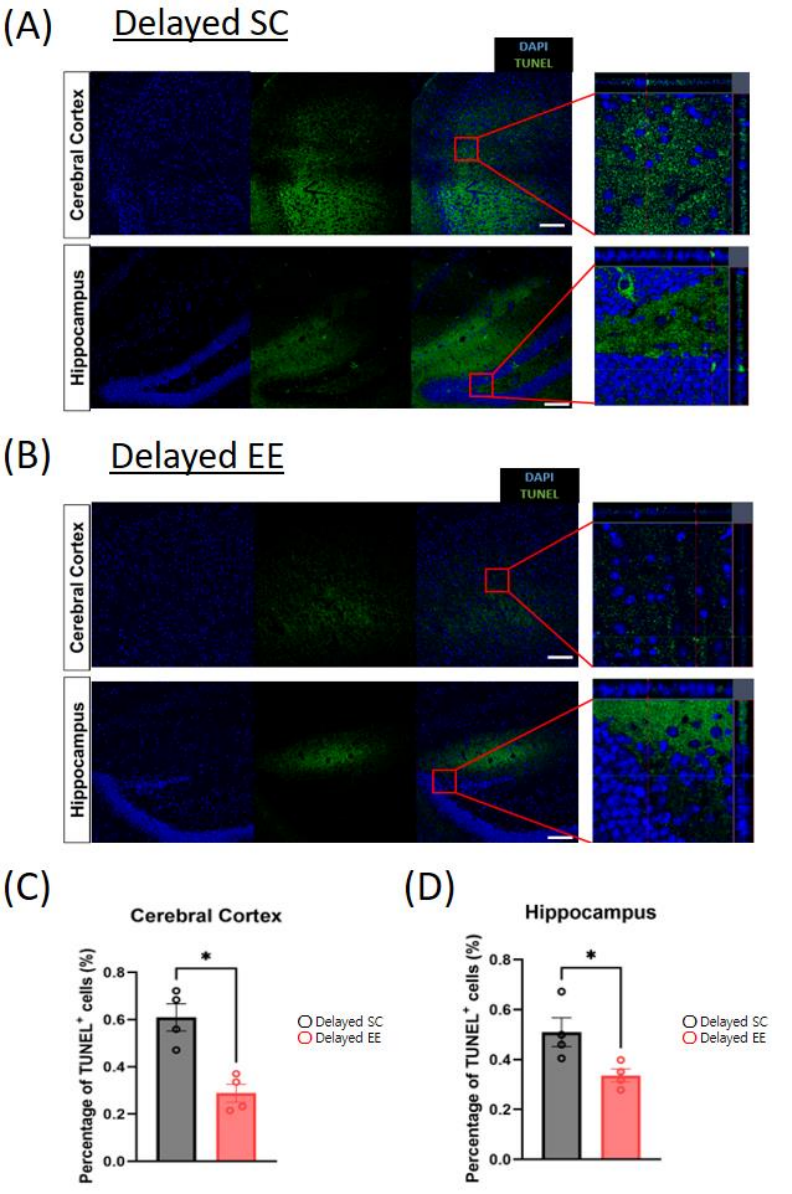

Figure 13. Delayed exposure to EE decreases DNA fragmentation of brain cells in cortex and hippocampus by inhibiting intrinsic apoptosis (SC, n = 4; EE, n = 4). TUNEL+ cells are indicated in green (A, B). The number of TUNEL+ cells in both cerebral cortex and hippocampus of EE mice decreased significantly compared with control mice (C, D; $p < 0.05$). Values are means ± SEM. An asterisk indicates significant difference (*$p < 0.05$ by Mann–Whitney U-test). Scale bars represent 100 μm.

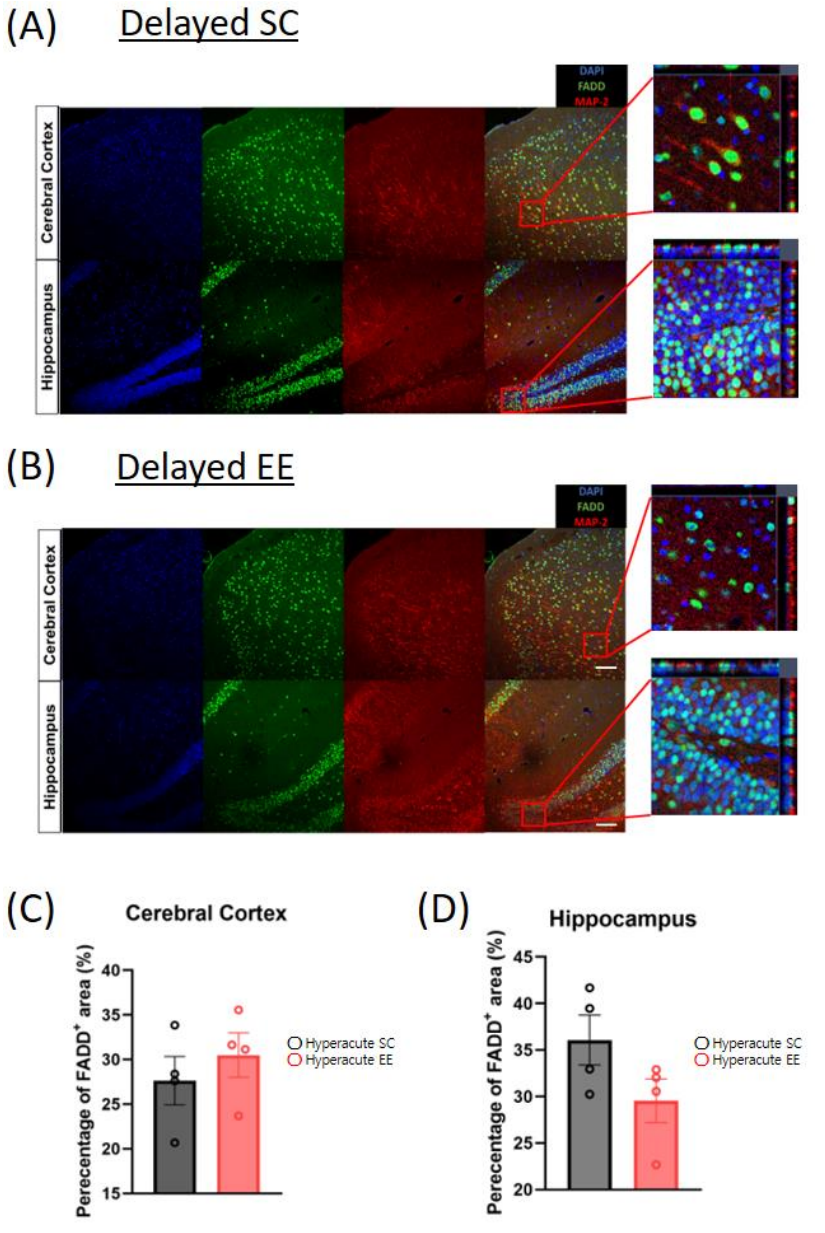

Figure 14. Delayed exposure to EE does not decrease extrinsic pathway-related neuronal apoptosis in cerebral cortex and hippocampus (SC, n = 4; EE, n = 4) FADD+ neurons are indicated in green (A, B). FADD+ cells in both cortex and hippocampus of mice exposed to delayed EE did not show significant differences compared with control mice (C, D). Values are means ± SEM. Scale bars represent 100 μm.

IV. DISCUSSION

Early mobilization post-stroke has been investigated extensively and is recommended by several clinical practice guidelines internationally because early initiation of exercise (24 to 72 h post-stroke) promotes functional recovery, prevents post-stroke complications, and facilitates return to society.[35, 36] However, exposure to high doses very early and forced exercise within 24 h post-stroke might adversely affect stroke outcomes. The effects of very early commencement of VE on functional recovery and the underlying mechanism after stroke have yet to be fully elucidated.

In the current study, hyperacute exposure to EE including VE significantly improved functional recovery and preserved neuronal survival. The neuroprotective effects were mediated via downregulation of both extrinsic and intrinsic signaling pathways of apoptosis. Especially, a significant downregulation of Fas/FasL-mediated apoptosis in cerebral cortex and hippocampus was detected in mice exposed to hyperacute EE compared with those subjected to delayed EE or SC.

Previous studies have shown that VE may improve motor and cognitive ability, and promoted anti-apoptotic as well as neuroprotective effects.[71, 72] Compared with forced exercise, VE is not associated with systemic stress and does not decrease the neuroprotective effect.[71,73,74] VE via exploratory movements such as EE may have greater benefit.[75] An early study demonstrated the beneficial effects of VE on hippocampal function, which were associated with suppression of cleaved caspase-3 expression, reduction of Bax expression and increased Bcl-2 expression in the hippocampus.[76,77] Following stroke, VE may improve motor rehabilitation, enhance cognitive ability and hippocampal BDNF expression compared with involuntary muscle movement and forced exercise.[74] The effects of voluntary movements post-stroke on neuronal regeneration and repair were related to upregulation of the expression of growth-associated protein 43 and neurotrophin 3.[72] A recent study reported that early commencement of VE post-stroke improved cerebral blood flow, vascular quality, functional connectivity, as well as white matter fiber density and

orientation in the brain, and improved motor abilities and overall activity.[78]

In terms of forced exercise post-stroke, mild-, moderate- and high-intensity exercise training initiated at various time points following stroke played a beneficial role.[79-86] Especially, mild- and moderate-intensity exercise enhanced neuroprotection compared with high-intensity exercise training.[82-86] However, a very early start of forced exercise post-stroke aggravated brain damage and apoptotic cell death, and triggered energy deficits along with generation of reactive oxygen species.[47]

Apoptosis may contribute significantly to neuronal death following brain ischemia; however, the time window for effective stroke rehabilitation including VE and the underlying mechanisms are not fully understood. To our knowledge, the current study was the first of its kind to investigate the effect of hyperacute exposure to EE on both extrinsic and intrinsic pathways of apoptosis in an adult mouse model of HI brain injury. Our data reveal that hyperacute (within 3 hours) exposure to EE post-stroke suppresses both extrinsic and intrinsic pathways of apoptosis in cerebral cortex and hippocampus. This may be due to the higher sensitivity of these brain areas to therapies that suppress neuronal apoptosis.[87-90] These results provide novel insights into the mechanisms underlying the neuroprotective effects of hyperacute EE treatment after ischemic stroke.

Previous studies highlighted the importance of suppressing the extrinsic pathway of apoptosis for favorable outcomes during the acute phase of ischemic stroke. Several molecules involved in the TNF/Fas family death receptor-mediated extrinsic pathway are increased, particularly in the ischemic penumbra, very early after focal cerebral ischemia, and remain elevated or continued to increase in experimental animal models.[19,20,91] Upregulation of the expression of Fas, FasL, and TNF-related apoptosis-inducing ligands was observed within 12 hours after cerebral ischemia and peaked between 24 and 48 hours in the post-ischemic rat brain, which coincides with the time course of apoptotic death in neuronal cells.[92] In patients with acute ischemic stroke, Fas-induced apoptosis in peripheral blood was activated in the first week after the onset, followed by a decrease towards the end of the acute period.[93] In a rodent model of ischemic stroke, acute treatment with edaravone was neuroprotective in transient focal

ischemia, and the mechanism involved suppression of the Fas/FasL signaling pathway.[25] Recently, very early treatment with zonisamide decreased morbidity by suppressing the expression of caspase-3, caspase-8, and calpain-1, and inhibiting the apoptosis of neuronal cells after cerebral ischemia injury.[13] Further, intranasal administration of a Fas-blocking peptide 12 hours post-ischemic stroke attenuated Fas-mediated apoptosis, decreased infarct volumes, and reduced neurologic deficits.[24] Importantly, a significant reduction in infarct volume occurred in hybrid mice expressing FasL dysfunction and in TNF knockout mice 24 hours after stroke.[19,92] However, the mechanism of suppression of extrinsic apoptosis mediated by EE treatment in the hyperacute phase of ischemic stroke has yet to be reported. In the current study, we found that hyperacute exposure to EE significantly suppressed extrinsic apoptosis via downregulation of Fas/FasL-mediated signaling in both cerebral cortex and hippocampus; however, the delayed exposure to EE failed to inhibit the apoptosis execution pathway.

The Fas/FasL system plays an important role in apoptosis during the acute phase in otherneurological disorders, and the current study findings were in accordance with previous studies.[26,27,31-34] In a mouse model of traumatic brain injury, a marked expression of Fas in the injured cortex and in the ipsilateral hippocampal CA2/3 regions of mouse brain was observed 24 hours after experimental brain injury.[94] Further, Fas and FasL were both localized to cortical neurons and astrocytes of rat brains for up to 72 hours after injury.[95] Both sFas and FasL were elevated in the CSF for several days following severe head trauma.[96,97] A recent human study reported increasing prevalence of Fas ranging from pre-season to post-season controls, and sub-concussion, with the highest prevalence observed in acute concussion up to 24-48 hours after injury.[80] Fas-mediated apoptosis of neurons occurred in mouse models of acute and subacute SCI and reduced apoptosis and neurological dysfunction were detected in Fas-deficient mice compared with control mice after SCI.[98]

Furthermore, the extrinsic pathway of apoptosis plays a critical role in the induction of apoptosis in non-neuronal cells, especially in the acute phase.[26,27,31-34] Previous

studies demonstrated the effects of extrinsic pathway of apoptosis in acute injury of lung, liver, heart, and kidney, and acute parasite infection. Liu et al reported that targeting long non-coding RNA MALAT1 and microRNA miR-181a-5p might be a potential option for the management of acute lung injury and acute respiratory distress syndrome by directly inhibiting the expression of FAS and early phase apoptosis.[27] Tiao et al. investigated the protective role of microRNA-29a in acute liver injury in a mouse model of obstructive jaundice, mediated at least partially by modulating the extrinsic rather than intrinsic pathway of apoptosis.[31] Furthermore, CD95 (AP0-1/Fas)-mediated apoptosis was shown to play an important role in the pathogenesis of fulminant hepatic failure in acute Wilson's disease.[32] FADD deletion attenuated cardiomyocyte death and improved cardiac function in acute myocardial ischemia/reperfusion injury.[99] Recently, the reduced Fas and FasL expression in CD4+ T cells was associated with let-7 microRNA expression, which significantly inhibited the apoptosis of these cells, and improved cell survival rates in patients with acute coronary syndrome.[26] Several previous reports indicated that Fas/FasL signaling mediated the pathogenesis of acute ischemic kidney injury via tubular apoptosis and necrosis, suggesting that the Fas/FasL system represents an effective therapeutic target in ischemic acute kidney injury.[34] Meanwhile, Fas/FasL signaling was shown to be the primary signaling pathway involved in adrenal apoptosis during experimental acute Trypanosoma cruzi infection. Moreover, at a molecular level, Fas was involved in the amplification of the intrinsic apoptotic pathway along with the Bcl-2 family of proteins including Bid and Bax.[33]

While most of the studies elucidating the possible mechanisms underlying the neuroprotective effect of EE intervention focused on the early phase of stroke, the importance of neuronal survival in the relatively late phase has been neglected. The current study found that delayed exposure to EE reduces infarct volume and DNA damage in brain cells, and thereby improved neurobehavioral function. This result is consistent with a previous study, which demonstrated sustained functional recovery following exposure to EE 5 days after onset, resulting in significant survival of hippocampal newborn cells in a rat stroke model.[100] Moreover, exposure to EE for 10

days strongly rescued the diabetic brain from neurodegenerative progression.[101] However, our study demonstrated that delayed exposure to EE does not significantly suppress apoptosis.

The limitation of our study is that the diverse potential mechanisms of neuronal cell death contributing to long-term neuroprotection and functional recovery after stroke were not investigated, given the complexity. Furthermore, EE positively contributes to improved behavioral recovery after stroke in young animals. A recent study reported that EE had a limited benefit on behavioral recovery of older rats compared with young rats.[102] Since stroke primarily affects mostly the elderly patients, the neuroprotective effects demonstrated in this study may not precisely be applicable to aged subjects. Additionally, ischemic stroke in humans occurs preferentially in patients of both sexes carrying multiple comorbidities requiring various treatments with complex interactions. In contrast, out study involved young, healthy, male inbred mice housed under ideal conditions. Therefore, it is highly desirable to investigate the effects of hyperacute exposure to EE in an aged animal model including both male and females with multiple comorbidities to demonstrate the clinical relevance to stroke rehabilitation. Although the mechanism of EE-induced inhibition of neuronal apoptosis requires further investigation, our study suggests that Fas/FasL-mediated apoptosis may be an important target underlying the neuroprotective effects of very early EE treatment after HI brain injury, contributing to improved emotional, cognitive, and locomotor performance post-stroke.

V. CONCLUSION

Hyperacute exposure to EE leads to downregulation of Fas/FasL-mediated apoptosis signaling in cerebral cortex and hippocampus resulting in neuroprotection and neuronal survival after HI brain injury, and recovery of emotional, cognitive, and locomotor function. However, the complex mechanisms of neuronal death in ischemic stroke and the discrepancy between young and aged subjects underscore the need for further investigation. Elucidation of altered apoptosis-related gene expression in the cerebral cortex and hippocampus following hyperacute exposure to EE provides new insights into the potential neuroprotective role of EE in the rehabilitation of patients diagnosed with ischemic stroke.

REFERENCES

1. Li Y, Huang L, Ma Q, Concepcion KR, Song MA, Zhang P, et al. Repression of the glucocorticoid receptor aggravates acute ischemic brain injuries in adult mice. Int. J. Mol. 2018;19(8):2428.

2. Katan M, Luft A. Global Burden of Stroke. Semin Neurol. 2018;38(2):208-11

3. Bernardo-Castro S, Albino I, Barrera-Sandoval ÁM, Tomatis F, Sousa JA, Martins E, et al. Therapeutic Nanoparticles for the Different Phases of Ischemic Stroke. Life. 2021;11(6):482.

4. Lee BY, Chon J, Kim H-S, Lee JH, Yun DH, Yoo SD, et al. Association between a polymorphism in CASP3 and CASP9 genes and ischemic stroke. Ann Rehabil Med. 2017;41(2):197.

5. Winstein CJ, Stein J, Arena R, Bates B, Cherney LR, Cramer SC, et al. Guidelines for adult stroke rehabilitation and recovery: a guideline for healthcare professionals from the American Heart Association/American Stroke Association. Stroke. 2016;47(6):e98-e169.

6. Radak D, Katsiki N, Resanovic I, Jovanovic A, Sudar-Milovanovic E, Zafirovic S, et al. Apoptosis and acute brain ischemia in ischemic stroke. Curr. Vasc. Pharmacol.. 2017;15(2):115-22.

7. Tuo Qz, Zhang St, Lei P. Mechanisms of neuronal cell death in ischemic stroke and their therapeutic implications. Med. Res. Rev. 2021.

8. Zhao H, Yenari MA, Cheng D, Barreto-Chang OL, Sapolsky RM, Steinberg GK. Bcl-2 transfection via herpes simplex virus blocks apoptosis-inducing factor translocation after focal ischemia in the rat. J. Cereb. Blood Flow Metab. 2004;24(6):681-92.

9. Singh MH, Brooke SM, Zemlyak I, Sapolsky RM. Evidence for caspase effects on release of cytochrome c and AIF in a model of ischemia in cortical neurons. Neurosci. Lett. 2010;469(2):179-83.

10. Zhang P, Zhang Y, Zhang J, Wu Y, Jia J, Wu J, et al. Early exercise protects against cerebral ischemic injury through inhibiting neuron apoptosis in cortex in rats. Int. J. Mol. Sci. 2013;14(3):6074-89.

11. Deng YH, He HY, Yang LQ, Zhang PY. Dynamic changes in neuronal autophagy and apoptosis in the ischemic penumbra following permanent ischemic stroke. Neural Regen. Res. 2016;11(7):1108.

12. Mitsios N, Gaffney J, Krupinski J, Mathias R, Wang Q, Hayward S, et al. Expression of signaling molecules associated with apoptosis in human ischemic stroke tissue. Cell Biochem. Biophys. 2007;47(1):73-85.

13. He J, Zhang X, He W, Xie Y, Chen Y, Yang Y, et al. Neuroprotective effects of zonisamide on cerebral ischemia injury via inhibition of neuronal apoptosis. Braz. J. Med. Biol. Res. 2021;54.

14. Bhardwaj A, Aggarwal BB. Receptor-mediated choreography of life and death. J. Clin. Immunol. 2003;23(5):317-32.

15. Schulze-Osthoff K, Ferrari D, Los M, Wesselborg S, Peter ME. Apoptosis signaling by death receptors. Eur J Biochem. 1998;254(3):439-59.

16. Love S. Apoptosis and brain ischaemia. Prog. Neuro-Psychopharmacol. Biol. Psychiatry. 2003;27(2):267-82.

17. Broughton BR, Reutens DC, Sobey CG. Apoptotic mechanisms after cerebral ischemia. Stroke. 2009;40(5):e331-e9.

18. Muhammad IF, Borné Y, Melander O, Orho-Melander M, Nilsson J, Söderholm M, et al. FADD (Fas-associated protein with death domain), caspase-3, and caspase-8 and incidence of ischemic stroke. Stroke. 2018;49(9):2224-6.

19. Rosenbaum DM, Gupta G, D'Amore J, Singh M, Weidenheim K, Zhang H, et al. Fas (CD95/APO-1) plays a role in the pathophysiology of focal cerebral ischemia. J. Neurosci. Res. 2000;61(6):686-92.

20. Chelluboina B, Klopfenstein JD, Gujrati M, Rao JS, Veeravalli KK. Temporal regulation of apoptotic and anti-apoptotic molecules after middle cerebral artery occlusion followed by reperfusion. Mol. Neurobiol. 2014;49(1):50-65.

21. Mahovic D, Zurak N, Lakusic N, Sporis D, Zarkovic N, Stancin N, et al. The dynamics of soluble Fas/APO 1 apoptotic biochemical marker in acute ischemic stroke patients. Adv Med Sci. 2013;58(2):298-303.

22. Rodhe J, Burguillos MA, de Pablos RM, Kavanagh E, Persson A, Englund E, et al. Spatio-temporal activation of caspase-8 in myeloid cells upon ischemic stroke. Acta Neuropathol. Commun. 2016;4(1):1-11.

23. Martin-Villalba A, Hahne M, Kleber S, Vogel J, Falk W, Schenkel J, et al. Therapeutic neutralization of CD95-ligand and TNF attenuates brain damage in stroke. Cell Death Differ. 2001;8(7):679-86.

24. Ullah I, Chung K, Oh J, Beloor J, Bae S, Lee SC, et al. Intranasal delivery of a Fas-blocking peptide attenuates Fas-mediated apoptosis in brain

ischemia. Sci. Rep. 2018;8(1):1-10.

25. Xiao B, Bi FF, Hu YQ, Tian FF, Wu ZG, Mujlli HM, et al. Edaravone neuroprotection effected by suppressing the gene expression of the Fas signal pathway following transient focal ischemia in rats. Neurotox. Res. 2007;12(3):155-62.

26. Zhao B, Zhang Z, Gui L, Xiang Y, Sun X, Huang L. MiR-let-7i inhibits CD4+ T cell apoptosis in patients with acute coronary syndrome. Adv. Clin. Exp. Med. official organ Wroclaw Medical University.

27. Liu Y, Wang X, Li P, Zhao Y, Yang L, Yu W, et al. Targeting MALAT1 and miRNA-181a-5p for the intervention of acute lung injury/acute respiratory distress syndrome. Respir. Med. 2020;175:106210.

28. Krajewska M, You Z, Rong J, Kress C, Huang X, Yang J, et al. Neuronal deletion of caspase 8 protects against brain injury in mouse models of controlled cortical impact and kainic acid-induced excitotoxicity. PloS one. 2011;6(9):e24341.

29. Yu WR, Fehlings MG. Fas/FasL-mediated apoptosis and inflammation are key features of acute human spinal cord injury: implications for translational, clinical application. Acta Neuropathol. 2011;122(6):747-61.

30. Henshall DC, Bonislawski DP, Skradski SL, Lan J-Q, Meller R, Simon RP. Cleavage of bid may amplify caspase-8-induced neuronal death following focally evoked limbic seizures. Neurobiol. Dis. 2001;8(4):568-80.

31. Tiao MM, Wang FS, Huang LT, Chuang JH, Kuo HC, Yang YL, et al. MicroRNA-29a protects against acute liver injury in a mouse model of obstructive jaundice via inhibition of the extrinsic apoptosis pathway. Apoptosis. 2014;19(1):30-41.

32. Strand S, Hofmann WJ, Grambihler A, Hug H, Volkmann M, Otto G, et al. Hepatic failure and liver cell damage in acute Wilson's disease involve CD95 (APO-1/Fas) mediated apoptosis. Nat. Med. 1998;4(5):588-93.

33. Pérez AR, Lambertucci F, González FB, Roggero EA, Bottasso OA, de Meis J, et al. Death of adrenocortical cells during murine acute T. cruzi infection is not associated with TNF-R1 signaling but mostly with the type II pathway of Fas-mediated apoptosis. Brain Behav. Immun. 2017;65:284-95.

34. Furuichi K, Kokubo S, Hara A, Imamura R, Wang Q, Kitajima S, et al. Fas ligand has a greater impact than TNF-α on apoptosis and inflammation in ischemic acute kidney injury. Nephron Extra. 2012;2(1):27-38.

35. Powers WJ, Rabinstein AA, Ackerson T, Adeoye OM, Bambakidis NC, Becker K, et al. 2018 guidelines for the early management of patients with acute ischemic stroke: a guideline for healthcare professionals from the American Heart Association/American Stroke Association. Stroke. 2018;49(3):e46-e99.

36. Kim DY, Kim YH, Lee J, Chang WH, Kim MW, Pyun SB, et al. Clinical practice guideline for stroke rehabilitation in Korea 2016. Brain Neurorehabil. 2017;10(Suppl 1).

37. Bernhardt J, Dewey H, Thrift A, Collier J, Donnan G. A very early rehabilitation trial for stroke (AVERT) phase II safety and feasibility. Stroke. 2008;39(2):390-6.

38. Sundseth A, Thommessen B, Rønning OM. Early mobilization after acute stroke. J. Stroke Cerebrovasc. Dis. 2014;23(3):496-9.

39. Langhorne P, Wu O, Rodgers H, Ashburn A, Bernhardt J. A Very Early Rehabilitation Trial after stroke (AVERT): a Phase III, multicentre, randomised controlled trial. Health Technol Assess (Winchester, England), 21(54), 1-120. 2017.

40. Yelnik AP, Quintaine V, Andriantsifanetra C, Wannepain M, Reiner P, Marnef H, et al. AMOBES (Active Mobility Very Early After Stroke) A Randomized Controlled Trial. Stroke. 2017;48(2):400-5.

41. Schnitzler A, Yelnik A, Wanepain M, Reiner P, Devailly J, Vicaut E. Active mobility early after stroke (AMOBES), 1 year follow-up. A randomised controlled trial. Ann. Phys. Rehabil. Med. 2018;61:e20.

42. Tong Y, Cheng Z, Rajah GB, Duan H, Cai L, Zhang N, et al. High Intensity Physical Rehabilitation Later Than 24 h Post Stroke Is Beneficial in Patients: A Pilot Randomized Controlled Trial (RCT) Study in Mild to Moderate Ischemic Stroke. Front. neurol. 2019;10.

43. Humm JL, Kozlowski DA, James DC, Gotts JE, Schallert T. Use-dependent exacerbation of brain damage occurs during an early post-lesion vulnerable period. Brain Res. 1998;783(2):286-92.

44. Kozlowski DA, James DC, Schallert T. Use-dependent exaggeration of neuronal injury after unilateral sensorimotor cortex lesions. J. Neurosci. 1996;16(15):4776-86.

45. Schallert T, Kozlowski DA, Humm JL, Cocke RR. Use-dependent structural events in recovery of function. Adv Neurol. 1997;73:229-38.

46. Li F, Shi W, Zhao EY, Geng X, Li X, Peng C, et al. Enhanced apoptosis

from early physical exercise rehabilitation following ischemic stroke. J. Neurosci. Res. 2017;95(4):1017-24.

47. Li F, Geng X, Khan H, Pendy Jr JT, Peng C, Li X, et al. Exacerbation of brain injury by post-stroke exercise is contingent upon exercise initiation timing. Front. Cell. Neurosci. 2017;11:311.

48. Xu L, Zhu L, Zhu L, Chen D, Cai K, Liu Z, et al. Moderate Exercise Combined with Enriched Environment Enhances Learning and Memory through BDNF/TrkB Signaling Pathway in Rats. Int. J. Environ. Res. Public Health. 2021;18(16):8283.

49. Van Praag H, Kempermann G, Gage FH. Neural consequences of enviromental enrichment. Nat. Rev. Neurosci. 2000;1(3):191.

50. Seo JH, Pyo S, Shin YK, Nam BG, Kang JW, Kim KP, et al. The Effect of Environmental Enrichment on Glutathione-Mediated Xenobiotic Metabolism and Antioxidation in Normal Adult Mice. Front Neurol. 2018;9:425.

51. Zhang Y, Xu D, Qi H, Yuan Y, Liu H, Yao S, et al. Enriched environment promotes post-stroke neurogenesis through NF-κB-mediated secretion of IL-17A from astrocytes. Brain Res. 2018;1687:20-31.

52. Monteiro BM, Moreira FA, Massensini AR, Moraes MF, Pereira GS. Enriched environment increases neurogenesis and improves social memory persistence in socially isolated adult mice. Hippocampus. 2014;24(2):239-48.

53. Leggio MG, Mandolesi L, Federico F, Spirito F, Ricci B, Gelfo F, et al. Environmental enrichment promotes improved spatial abilities and enhanced dendritic growth in the rat. Behav. Brain Res. 2005;163(1):78-90.

54. He S, Ma J, Liu N, Yu X. Early enriched environment promotes neonatal GABAergic neurotransmission and accelerates synapse maturation. J. Neurosci. 2010;30(23):7910-6.

55. Zhang X, Chen XP, Lin JB, Xiong Y, Liao WJ, Wan Q. Effect of enriched environment on angiogenesis and neurological functions in rats with focal cerebral ischemia. Brain Res. 2017;1655:176-85.

56. Song SY, Pyo S, Choi S, Oh HS, Seo JH, Yu JH, et al. Environmental Enrichment Enhances Cav 2.1 Channel-Mediated Presynaptic Plasticity in Hypoxic–Ischemic Encephalopathy. Int. J. Mol. Sci. 2021;22(7):3414.

57. Kraeuter AK, Guest PC, Sarnyai Z. The Open Field Test for Measuring

Locomotor Activity and Anxiety-Like Behavior. Methods Mol Biol. 2019;1916:99-103.

58. Kim K, Wi S, Seo JH, Pyo S, Cho S-R. Reduced Interaction of Aggregated α-Synuclein and VAMP2 by Environmental Enrichment Alleviates Hyperactivity and Anxiety in a Model of Parkinson's Disease. Genes. 2021;12(3):392.

59. Conn PM. Animal models for the study of human disease: Academic Press; 2017.

60. Nishigaki R, Yokoyama Y, Shimizu Y, Marumoto R, Misumi S, Ueda Y, et al. Monosodium glutamate ingestion during the development period reduces aggression mediated by the vagus nerve in a rat model of attention deficit-hyperactivity disorder. Brain Res. 2018;1690:40-50.

61. Metz GA, Whishaw IQ. The ladder rung walking task: a scoring system and its practical application. J Vis Exp. 2009(28).

62. Seo JH, Yu JH, Suh H, Kim MS, Cho SR. Fibroblast growth factor-2 induced by enriched environment enhances angiogenesis and motor function in chronic hypoxic-ischemic brain injury. PLoS One. 2013;8(9):e74405.

63. Wahl F, Allix M, Plotkine M, Boulu RG. Neurological and behavioral outcomes of focal cerebral ischemia in rats. Stroke. 1992;23(2):267-72.

64. Lee EJ, Malik A, Pokharel S, Ahmad S, Mir BA, Cho KH, et al. Identification of genes differentially expressed in myogenin knock-down bovine muscle satellite cells during differentiation through RNA sequencing analysis. PloS one. 2014;9(3):e92447.

65. Kim WJ, Lee SH, An SB, Kim SE, Liu Q, Choi JY, et al. Comparative transcriptome analysis of queen, worker, and larva of Asian honeybee, apis cerana. Int. J. Ind. Entomol. 2013;27(2):271-6.

66. Kim MS, Yu JH, Lee MY, Kim AL, Jo MH, Kim M, et al. Differential expression of extracellular matrix and adhesion molecules in fetal-origin amniotic epithelial cells of preeclamptic pregnancy. PLoS One. 2016;11(5):e0156038.

67. Karthik L, Kumar G, Keswani T, Bhattacharyya A, Chandar SS, Bhaskara Rao K. Protease inhibitors from marine actinobacteria as a potential source for antimalarial compound. PloS one. 2014;9(3):e90972.

68. Kim JH, Jeon M, Song JS, Lee JH, Choi BJ, Jung HS, et al. Distinctive genetic activity pattern of the human dental pulp between deciduous and

permanent teeth. PloS one. 2014;9(7):e102893.

69. Duan WR, Garner DS, Williams SD, Funckes-Shippy CL, Spath IS, Blomme EA. Comparison of immunohistochemistry for activated caspase-3 and cleaved cytokeratin 18 with the TUNEL method for quantification of apoptosis in histological sections of PC-3 subcutaneous xenografts. J Pathol. 2003;199(2):221-8.

70. Wi S, Lee JW, Kim M, Park CH, Cho SR An Enriched Environment Ameliorates Oxidative Stress and Olfactory Dysfunction in Parkinson's Disease with α-Synucleinopathy. Cell Transplant. 2018;27(5):831-9.

71. Mokhtari-Zaer A, Ghodrati-Jaldbakhan S, Vafaei AA, Miladi-Gorji H, Akhavan MM, Bandegi AR, et al. Effects of voluntary and treadmill exercise on spontaneous withdrawal signs, cognitive deficits and alterations in apoptosis-associated proteins in morphine-dependent rats. Behav Brain Res. 2014;271:160

72. Xing Y, Yang SD, Dong F, Wang MM, Feng Y-S, Zhang F. The beneficial role of early exercise training following stroke and possible mechanisms. Life sci. 2018;198:32-7.

73. Yanagita S, Amemiya S, Suzuki S, Kita I. Effects of spontaneous and forced running on activation of hypothalamic corticotropin-releasing hormone neurons in rats. Life Sci. 2007;80(4):356-63.

74. Ke Z, Yip SP, Li L, Zheng XX, Tong KY. The effects of voluntary, involuntary, and forced exercises on brain-derived neurotrophic factor and motor function recovery: a rat brain ischemia model. PloS one. 2011;6(2):e16643.

75. Biernaskie J, Corbett D. Enriched rehabilitative training promotes improved forelimb motor function and enhanced dendritic growth after focal ischemic injury. J Neurosci. 2001;21(14):5272-80.

76. Ko YJ, Ko IG. Voluntary wheel running improves spatial learning memory by suppressing inflammation and apoptosis via inactivation of nuclear factor kappa B in brain inflammation rats. Int Neurourol J. 2020;24(Suppl 2):96.

77. Van Praag H. Exercise and the brain: something to chew on. Trends Neurosci. 2009;32(5):283-90.

78. Lohkamp KJ, Kiliaan AJ, Shenk J, Verweij V, Wiesmann M. The impact of voluntary exercise on stroke recovery. Front neurosci. 2021:856.

79. Pin E, Petricoin EF, Cortes N, Bowman TG, Andersson E, Uhlen M, et al.

Immunoglobulin A Autoreactivity toward Brain Enriched and Apoptosis-Regulating Proteins in Saliva of Athletes after Acute Concussion and Subconcussive Impacts. J Neurotrauma. 2021;38(17):2373-83.

80. Bell JA, Wolke ML, Ortez RC, Jones TA, Kerr AL. Training intensity affects motor rehabilitation efficacy following unilateral ischemic insult of the sensorimotor cortex in C57BL/6 mice. Neurorehabil Neural Repair. 2015;29(6):590-8.

81. Wang Q, Wang P, Meng P, Han C, Yue S. Intensive training accelerates the recovery of motor functions following cerebral ischemia-reperfusion in MCAO rats. Eur Rev Med Pharmacol Sci. 2016;20(18):3839-52.

82. Lee SU, Kim DY, Park SH, Choi DH, Park HW, Han TR. Mild to moderate early exercise promotes recovery from cerebral ischemia in rats. Can J Neurol Sci. 2009;36(4):443-9.

83. Leasure JL, Grider M. The effect of mild post-stroke exercise on reactive neurogenesis and recovery of somatosensation in aged rats. Exp Neurol. 2010;226(1):58-67.

84. Zhang A, Bai Y, Hu Y, Zhang F, Wu Y, Wang Y, et al. The effects of exercise intensity on p-NR2B expression in cerebral ischemic rats. Can J Neurol Sci. 2012;39(5):613-8.

85. Shih PC, Yang YR, Wang RY. Effects of exercise intensity on spatial memory performance and hippocampal synaptic plasticity in transient brain ischemic rats. PloS one. 2013;8(10):e78163.

86. Sun J, Ke Z, Yip SP, Hu XL, Zheng XX, Tong KY. Gradually increased training intensity benefits rehabilitation outcome after stroke by BDNF upregulation and stress suppression. Biomed Res Int. 2014;2014 :925762.

87. Chen X, Zhang X, Xue L, Hao C, Liao W, Wan Q. Treatment with enriched environment reduces neuronal apoptosis in the periinfarct cortex after cerebral ischemia/reperfusion injury. Cell. Physiol. Biochem.. 2017;41(4):1445-56.

88. Seo TB, Kim TW, Shin MS, Ji ES, Cho HS, Lee JM, et al. Aerobic exercise alleviates ischemia-induced memory impairment by enhancing cell proliferation and suppressing neuronal apoptosis in hippocampus. Int. Neurourol. J. 2014;18(4):187.

89. Cho YS, Shin MS, Ko IG, Kim SE, Kim CJ, Sung YH, et al. Ulinastatin inhibits cerebral ischemia-induced apoptosis in the hippocampus of gerbils. Mol. Med. Rep. 2015;12(2):1796-802.

90. Zhang W, Wen J, Jiang Y, Hu Q, Wang J, Wei S, et al. l-Borneol ameliorates cerebral ischaemia by downregulating the mitochondrial calcium uniporter-induced apoptosis cascade in pMCAO rats. J. Pharm. Pharmacol. 2021;73(2):272-80.

91. Dzietko M, Boos V, Sifringer M, Polley O, Gerstner B, Genz K, et al. A critical role for Fas/CD-95 dependent signaling pathways in the pathogenesis of hyperoxia-induced brain injury. Ann Neurol. 2008;64(6):664-73.

92. Martin-Villalba A, Herr I, Jeremias I, Hahne M, Brandt R, Vogel J, et al. CD95 ligand (Fas-L/APO-1L) and tumor necrosis factor-related apoptosis-inducing ligand mediate ischemia-induced apoptosis in neurons. J Neurosci. 1999;19(10):3809-17.

93. Sergeeva S, Savin A, Litvitsky P, Lyundup A, Breslavich I, Manasova ZS. Neurohumoral response and Fas-ligand-induced apoptosis in peripheral blood of patients with acute ischemic stroke. Zh Nevrol Psikhiatr Im S S Korsakova. 2020;120(6):57-63.

94. Grosjean M, Lenzlinger P, Stahel P, Yatsiv I, Shohami E, Trentz O, et al. Immunohistochemical characterization of Fas (CD95) and Fas Ligand (FasL-CD95L) expression in the injured brain: Relationship with neuronal cell death and inflammatory mediators. Histol Histopathol. 2007.

95. Beer R, Gerhard F, Schöpf M, Reindl M, Zelger B, Schmutzhard E, et al. Expression of Fas and Fas ligand after experimental traumatic brain injury in the rat. J Cereb Blood Flow Metab. 2000;20(4):669-77.

96. Ertel W, Keel M, Stocker R, Imhof H-G, Leist M, Steckholzer U, et al. Detectable concentrations of Fas ligand in cerebrospinal fluid after severe head injury. J Neuroimmunol. 1997;80(1-2):93-6.

97. Lenzlinger PM, Hans VH, Joller-Jemelka HI, Trentz O, Morganti-Kossmann MC, Kossmann T. Markers for cell-mediated immune response are elevated in cerebrospinal fluid and serum after severe traumatic brain injury in humans. J Neurotrauma. 2001;18(5):479-89.

98. Yu WR, Fehlings MG. Fas/FasL-mediated apoptosis and inflammation are key features of acute human spinal cord injury: implications for translational, clinical application. Acta Neuropathol. 2011; 122(6):747-61

99. Fan Q, Huang ZM, Boucher M, Shang X, Zuo L, Brinks H, et al. Inhibition of Fas-associated death domain-containing protein (FADD) protects against myocardial ischemia/reperfusion injury in a heart failure mouse model. PLoS One. 2013;8(9):e73537.

100. Tang Y, Li MY, Zhang X, Jin X, Liu J, Wei PH. Delayed exposure to environmental enrichment improves functional outcome after stroke. J Pharmacol Sci. 2019;140(2):137-43.

101. Beauquis J, Roig P, De Nicola AF, Saravia F. Short-term environmental enrichment enhances adult neurogenesis, vascular network and dendritic complexity in the hippocampus of type 1 diabetic mice. PloS one. 2010;5(11):e13993.

102. Gresita A, Mihai R, Hermann DM, Amandei FS, Capitanescu B, Popa-Wagner A. Effect of environmental enrichment and isolation on behavioral and histological indices following focal ischemia in old rats. Geroscience. 2021:1-18.

ABSTRACT (IN KOREAN)

저산소성-허혈성 뇌손상에서 초급성기 부유 환경 재활치료가 미치는 신경학적, 기능적 영향 및 유전자 발현 프로파일링 분석

<지도교수 박중현>

연세대학교 대학원 의학과

이 후 영

뇌졸중은 사망률이 높고 후유증도 심각한 질환이다. 세포사멸은 뇌졸중의 병태생리에 중요한 역할을 하며 뇌졸중 급성기에 FAS 등 외인적 세포사멸과 관련된 단백질의 발현이 증가한다는 이전 연구 결과들이 보고된 바 있다.

뇌졸중 발생 후 조기재활 치료는 환자의 기능회복, 합병증 예방, 조기 복귀에 중요한 것으로 보고되고 있으며, 국내외 매우 많은 임상지침에서 제안되고 있으나 뇌졸중 발병 24시간 이내에 다빈도, 고용량, 초조기(very early) 활동은 표준치료와 비교하였을 때 양호한 결과의 비가 감소되는 것과 관련이 있었다. 하지만 자발적 운동을 포함한 부유 환경을 초조기에 노출하였을 때 신경행동학적 회복에 미치는 영향과 그 기전은 밝혀지지 않았다.

부유 환경이란 대형 쥐 사육장(예:86×76cm)에 사회적 상호작용을 위해 여러 마리의 집단(예:12~13마리)을 다양한 장난감, 나무조각, 터널 등을 배치하고 위치를 자주 변화시키며, 자발적 운동을 위해 수레바퀴를 설치한 후 사육하는 환경이다. 본 연구의 목적은 초급성기 저산소-허혈성 뇌손상 성인 쥐 모델에서 부유환경 노출이 신경행동학적으로 미치는 영향을 알아보고자

하였으며 분자, 조직학적 기전이 세포사멸을 조절하는 유전자 및 단백질 발현을 조절하는 효과가 있는지 밝히고자 하였다.

뇌졸중 후 초급성기 재활 동물 모델을 구현하기 위하여 총 70마리의 6주령 C57Bl/6 마우스에 저산소성 허혈성 뇌손상을 가한 후 3시간 이내로 표준 사육장 또는 부유환경(그룹당 35 마리) 중 하나에 무작위로 배정한 후 2주 동안 노출시켰다. 불안과 운동기능을 평가하기 위해 오픈필드 테스트를 실시하였고, 불안과 과활동성을 평가하기 위해 실린더 테스트를 실시하였다. 이후 공간 기억력을 평가하기 위해 Y 미로 테스트를 실시하였고, 이동성 운동기능을 평가하기 위하여 래더 워킹 테스트를 실시하였다. 부유환경 초급성기 노출이 끼치는 분자적 기전에 대한 영향을 밝히기 위하여 대뇌피질과 해마에서 차등 발현 유전자를 전사체분석을 통하여 분석하였다. 이러한 유전자와 관련된 단백질의 발현을 검증하기 위해 웨스턴 블랏을 실시하였으며 면역조직화학염색법을 이용한 조직학적 분석을 실시하였다. 그리고 뇌졸중 후 지연된 재활 동물 모델과 비교하기 위하여 총 40마리의 6주령 C57Bl/6 마우스에 저산소성 허혈성 뇌손상을 가한 후 3일 후 표준 사육장 또는 부유환경(그룹당 20 마리) 중 하나에 무작위로 배정한 후 2주 동안 노출시켰다. 그리고 초급성기 부유환경 노출 동물모델에서 실시한 신경행동학적 검사, 분자적 검사, 그리고 조직학적 검사를 지연된 부유환경 노출 동물모델에서도 실시하였다.

행동 평가 결과 초급성기에 부유환경에 노출된 저산소성-허혈성 뇌손상 쥐는 표준 사육장에 노출된 대조군 쥐와 비교하여 오픈필드 테스트에서 총 이동 거리가 유의하게 감소하며 불안이 유의하게 완화되었으며, Y-미로 검사에서 유의한 인지기능의 호전이 관찰되었고, 래더 워킹 테스트에서 미끄러짐이 유의하게 감소하며 이동성 운동기능의 유의한 호전을 보였다. 전사체 분석 결과, 초급성기에 부유환경에 노출된 마우스의 대뇌피질과 해마에서 차등 발현된 유전자가 외인적 세포사멸 경로의 조절과 관련이 있으며 FAS와 CASP8이 유의하게 하향 발현되었다.

웨스턴 블랏 분석에서는 대조군과 비교하여 부유환경에 초급성기에 노출된 마우스의 대뇌피질과 해마에서 FADD, FAS, Bax 및 cleaved caspase-8/caspase-8 비율, Bax/Bcl-2 비율, 그리고 cleaved caspase-3/caspase-3 비율이 유의하게 감소하였다. 면역조직화학염색 결과 부유환경에 초급성기에 노출된 저산소성-허혈성 뇌손상 마우스에서 TUNNEL+와 MAP-2+ /FADD+에 염색된 세포 및 뉴런이 대조군과 비교하여 유의하게 감소하였다.

저산소성-허혈성 뇌손상 후 부유환경에 노출이 지연된 군에서는 표준 사육장에 노출된 대조군 쥐와 비교하여 불안, 인지기능 및 운동기능의 유의한 호전을 보였다. 웨스턴 블랏 분석에서는 대조군과 비교하여 부유환경 노출이 지연된 마우스의 대뇌피질과 해마에서 세포사멸을 유의하게 억제하는 효과는 관찰되지 않았다. 면역조직화학염색 결과 부유환경에 지연 노출된 마우스에서 TUNNEL+에 염색된 세포는 대조군과 비교하여 유의하게 감소하였으나 FADD+ 염색된 뉴론의 수는 유의한 변화가 관찰되지 않았다.

결론적으로 저산소성-허혈성 뇌손상 후 초급성기에 자발운동이 포함된 부유환경에 노출되면 대뇌피질과 해마의 외인적 세포사멸과 더불어 내인적인 세포사멸이 유의하게 감소한다. FAS와 CASP8 하향 조절과 같은 외인적 세포사멸과 관련된 유전자 프로파일 발현의 변화는 저산소성-허혈성 뇌손상 후 초급성기 부유환경 노출이 신경보호 효과 및 정서, 인지, 그리고 운동 기능 회복과 연관이 있음을 시사한다.

핵심되는 말 : 부유환경, 저산소성-허혈성 뇌손상, 뇌졸중, 세포사멸, FAS, 외인적 경로, 기능 회복, 초급성기

PUBLICATION LIST

(1) Lee, H. Y., Park, J. H., Kim, A. R., Park, M., & Kim, T. W. (2020). Neurobehavioral recovery in patients who emerged from prolonged disorder of consciousness: a retrospective study. BMC neurology, 20, 1-11.

(2) Lee, H. Y., Park, J. H., Lee, H., Kim, T. W., & Yoo, S. D. (2020). Does hip bone density differ between paretic and non-paretic sides in hemiplegic stroke patients? And its relationship with physical impairment. Journal of Bone Metabolism, 27(4), 237.

(3) Lee, H. Y., Park, J. H., & Kim, T. W. (2021). Cross-cultural adaptation and psychometric validation of the Korean version of rehabilitation complexity scale for the measurement of complex rehabilitation needs. Medicine, 100(24).

(4) Lee, H. Y., Park, J. H., & Kim, T. W. (2021). Comparisons between Locomat and Walkbot robotic gait training regarding balance and lower extremity function among non-ambulatory chronic acquired brain injury survivors. Medicine, 100(18).